

# Comparative orbital evolution of transient Uranian co-orbitals: exploring the role of ephemeral multibody mean motion resonances

C. de la Fuente Marcos<sup>\*</sup> and R. de la Fuente Marcos

*Universidad Complutense de Madrid, Ciudad Universitaria, E-28040 Madrid, Spain*

Accepted 2014 April 9. Received 2014 April 7; in original form 2014 February 17

## ABSTRACT

Uranus has three known co-orbitals: 83982 Crantor (2002 GO<sub>9</sub>), 2010 EU<sub>65</sub> and 2011 QF<sub>99</sub>. All of them were captured in their current resonant state relatively recently. Here, we perform a comparative analysis of the orbital evolution of these transient co-orbitals to understand better how they got captured in the first place and what makes them dynamically unstable. We also look for additional temporary Uranian co-orbital candidates among known objects. Our  $N$ -body simulations show that the long-term stability of 2011 QF<sub>99</sub> is controlled by Jupiter and Neptune; it briefly enters the 1:7 mean motion resonance with Jupiter and the 2:1 with Neptune before becoming a Trojan and prior to leaving its tadpole orbit. During these ephemeral two-body mean motion resonance episodes, apsidal corotation resonances are also observed. For known co-orbitals, Saturn is the current source of the main destabilizing force but this is not enough to eject a minor body from the 1:1 commensurability with Uranus. These objects must enter mean motion resonances with Jupiter and Neptune in order to be captured or become passing Centaurs. Asteroid 2010 EU<sub>65</sub>, a probable visitor from the Oort cloud, may have been stable for several Myr due to its comparatively low eccentricity. Additionally, we propose 2002 VG<sub>131</sub> as the first transient quasi-satellite candidate of Uranus. Asteroid 1999 HD<sub>12</sub> may signal the edge of Uranus' co-orbital region. Transient Uranian co-orbitals are often submitted to complex multibody ephemeral mean motion resonances that trigger the switching between resonant co-orbital states, making them dynamically unstable. In addition, we show that the orbital properties and discovery circumstances of known objects can be used to outline a practical strategy by which additional Uranus' co-orbitals may be found.

**Key words:** celestial mechanics – minor planets, asteroids: individual: 1999 HD<sub>12</sub> – minor planets, asteroids: individual: 83982 Crantor (2002 GO<sub>9</sub>) – minor planets, asteroids: individual: 2002 VG<sub>131</sub> – minor planets, asteroids: individual: 2010 EU<sub>65</sub> – minor planets, asteroids: individual: 2011 QF<sub>99</sub> – planets and satellites: individual: Uranus.

## 1 INTRODUCTION

Besides bound companions or natural satellites, planets may have unbound companions or co-orbitals, i.e. objects trapped in a 1:1 mean motion resonance with the planet. Co-orbital bodies are not only interesting curiosities found in the celestial mechanics studies, but also represent temporary reservoirs for certain objects as well as the key to understand the origin of retrograde outer satellites of the giant planets and the accretional processes in the early Solar system (see e.g. Namouni, Christou & Murray 1999). These co-orbital bodies can be primordial, if they were captured in their present resonant state early in the history of the Solar system and have remained dynamically stable for billions of years, or transient, if they were captured relatively recently.

Several thousand minor bodies are known to be currently trapped in the 1:1 mean motion resonance with Jupiter and most of

them may have remained as such for Gyr (see e.g. Milani 1993; Jewitt, Trujillo & Luu 2000; Morbidelli et al. 2005; Yoshida & Nakamura 2005; Robutel & Gabern 2006; Robutel & Bodossian 2009; Grav et al. 2011; Nesvorný, Vokrouhlický & Morbidelli 2013). Neptune also hosts a likely large population of co-orbitals both long-term stable (e.g. Kortenkamp, Malhotra & Michtchenko 2004; Nesvorný & Vokrouhlický 2009; Sheppard & Trujillo 2006, 2010) and transient (e.g. de la Fuente Marcos & de la Fuente Marcos 2012b,c). In sharp contrast, the number of asteroids currently engaged in co-orbital motion with Uranus appears to be rather small and its nature comparatively ephemeral. Uranus has Centaurs temporarily trapped in other mean motion resonances as well (Masaki & Kinoshita 2003; Gallardo 2006, 2014).

The theoretical possibility of finding primordial or transient Uranian co-orbitals, in particular Trojans, has been a subject of study for almost three decades. In general, numerical simulations predict that Uranus may have retained a certain amount of its primordial co-orbital minor planet population and also that short-term

<sup>\*</sup> E-mail: nbplanet@fis.ucm.es

stable (for some Myr) co-orbitals may exist. Zhang & Innanen (1988a,b) and Innanen & Mikkola (1989) found that some tadpole orbits may survive for 10 Myr. Mikkola & Innanen (1992) described tadpole orbits stable for at least 20 Myr and with libration amplitudes close to  $100^\circ$ ; horseshoe orbiters were only stable for shorter periods of time ( $<10$  Myr). Holman & Wisdom (1993) found similar results. Gomes (1998) explained the observational absence of primordial Uranus Trojans as a side effect of planetary migration. Wiegert, Innanen & Mikkola (2000) focused on quasi-satellites and found that some test orbits were stable for up to 1 Gyr but only at low inclinations ( $<2^\circ$ ) and with eccentricities in the range 0.1–0.15. Nesvorný & Dones (2002) concluded that any existing Uranus' primordial Trojan population should have now been depleted by a factor of 100. Gacka (2003) also found short-term stable tadpole orbits. In a very detailed study, Marzari, Tricarico & Scholl (2003) identified a real absence of Trojan stable orbits at low libration amplitudes and also that, among the Jovian planets, Uranus has the lowest probability of hosting long-term stable Trojans. Horner & Evans (2006) stated that Uranus appears not to be able to efficiently capture objects into the 1:1 commensurability today even for short periods of time. Lykawka & Horner (2010) found that Uranus should have been able to capture and retain a significant population of Trojan objects from the primordial planetesimal disc by the end of planetary migration. These authors concluded that originally the orbits of these objects should have had a wide range of orbital eccentricities and inclinations.

Predictions from numerical simulations appear to be generally consistent with the available observational evidence that transient Uranian co-orbitals do exist but primordial ones may not. So far, Uranus has only three known co-orbitals: 83982 Crantor (2002 GO<sub>9</sub>) (Gallardo 2006; de la Fuente Marcos & de la Fuente Marcos 2013b), 2010 EU<sub>65</sub> (de la Fuente Marcos & de la Fuente Marcos 2013b) and 2011 QF<sub>99</sub> (Alexandersen et al. 2013a; Alexandersen et al. 2013b). Due to its present short data-arc (85 d), 2010 EU<sub>65</sub> is better described as a candidate. Asteroids Crantor and 2010 EU<sub>65</sub> follow horseshoe orbits in a frame of reference rotating with Uranus and 2011 QF<sub>99</sub> is an L<sub>4</sub> Trojan; the three of them are only short-term stable and, therefore, they must be captured objects. Most published studies focus on what makes a hypothetical primordial population of Uranian co-orbitals dynamically unstable, leaving the question of how the transient ones got captured unanswered.

In absence of observational bias, the lack of a sizeable present-day population of minor bodies trapped in the 1:1 commensurability with Uranus is probably due to persistent perturbations by the other giant planets. Uranus' Trojans are affected by high-order resonances with Saturn (Gallardo 2006). In the case of current horseshoe librators, Saturn also appears to be the main source of the destabilizing force (de la Fuente Marcos & de la Fuente Marcos 2013b). Dvorak, Bazsó & Zhou (2010) studied the stability of hypothetical primordial Uranus' Trojans and concluded that the Trojan regions are mostly unstable. For these authors, the orbital inclination is the key parameter to characterize the stability of Uranus' Trojans; only the inclination intervals  $(0, 7)^\circ$ ,  $(9, 13)^\circ$ ,  $(31, 36)^\circ$  and  $(38, 50)^\circ$  appear to be stable (regions A, B, C and D, respectively, in Dvorak et al. 2010). The existence of these islands of stability enables the presence of Trojan companions to Uranus. Asteroid 2011 QF<sub>99</sub> appears to inhabit one of these stable areas in orbital parameter space as its current orbital inclination is nearly  $11^\circ$  but it is not a primordial Uranus' Trojan.

Here, we revisit the subjects of capture and stability of current Uranian co-orbitals, providing an independent assessment of the 1:1 commensurability of the newly found Uranus' Trojan,

2011 QF<sub>99</sub>, studying its future orbital evolution and looking into its dynamical past. Our numerical investigation is aimed at adding more pieces to the overall puzzle of the apparent scarcity of Uranian co-orbitals as we explore the role of multibody ephemeral mean motion resonances. On the other hand, the comparative study of both the dynamics of the few known co-orbitals and candidates, and their discovery circumstances, reveals important additional clues to solve this puzzle. This paper is organized as follows. In Section 2, we briefly discuss the numerical model used in our  $N$ -body simulations. The current status of 2011 QF<sub>99</sub> is reviewed in Section 3. The capture mechanism and stability of 2011 QF<sub>99</sub> are further studied in Section 4. We revisit the cases of Crantor and 2010 EU<sub>65</sub> in Section 5. Section 6 introduces a few new Uranus' co-orbital candidates. In Section 7, we discuss our results on the stability of current Uranian co-orbitals. We present a practical guide to discover additional objects in Section 8. Section 9 summarizes our conclusions.

## 2 NUMERICAL INTEGRATIONS

In order to perform a comparative analysis of the orbital evolution of known transient Uranian co-orbitals, we solve directly the Newtonian equations of motion by means of the Hermite integration scheme described by Makino (1991) and implemented by Aarseth (2003). The adequacy of this integration approach for Solar system dynamical studies has been extensively tested by the authors (de la Fuente Marcos & de la Fuente Marcos 2012a,b,c, 2013a,b). The standard version of this  $N$ -body sequential code is publicly available from the IoA web site<sup>1</sup>.

Our calculations include the perturbations by the eight major planets, the Moon, the barycentre of the Pluto-Charon system and the three largest asteroids, (1) Ceres, (2) Pallas and (4) Vesta. For accurate initial positions and velocities, we used the latest Heliocentric ecliptic Keplerian elements provided by the Jet Propulsion Laboratory (JPL) online Solar system data service<sup>2</sup> (Giorgini et al. 1996) and initial positions and velocities based on the DE405 planetary orbital ephemerides (Standish 1998) referred to the barycentre of the Solar system. The orbits were computed 1 Myr forward and backward in time. Additional details can be found in de la Fuente Marcos & de la Fuente Marcos (2012a).

In addition to the orbital calculations completed using the nominal elements in Tables 1 and 2, we have performed 50 control simulations with sets of orbital elements obtained from the nominal ones and the quoted uncertainties. These control orbits follow a Gaussian distribution in the six-dimensional space of orbital elements and their orbital parameters are compatible with the observations within the  $3\sigma$  uncertainties (see Tables 1 and 2), reflecting the observational incertitude in astrometry. In the integrations, the relative error in the total energy was always as low as  $2.0 \times 10^{-15}$  or lower after a simulated time of 1 Myr. The corresponding error in the total angular momentum is several orders of magnitude smaller. In all the figures, and unless explicitly stated,  $t = 0$  coincides with the JD2456800.5 epoch.

## 3 2011 QF<sub>99</sub>: A REVIEW

Asteroid 2011 QF<sub>99</sub> was discovered on 2011 August 29 at  $r = 22.6$  mag by M. Alexandersen observing from Mauna Kea with

<sup>1</sup> <http://www.ast.cam.ac.uk/~sverre/web/pages/nbody.htm>

<sup>2</sup> [http://ssd.jpl.nasa.gov/?planet\\_pos](http://ssd.jpl.nasa.gov/?planet_pos)

**Table 1.** Heliocentric Keplerian orbital elements of 2011 QF<sub>99</sub> used in this research. Values include the  $1\sigma$  uncertainty. The orbit is based on 29 observations spanning a data-arc of 419 d (Epoch = JD2456800.5, 2014-May-23.0; J2000.0 ecliptic and equinox. Source: JPL Small-Body Database).

Semimajor axis, $a$ (au)	=	$19.132 \pm 0.013$
Eccentricity, $e$	=	$0.178 \pm 0.002$
Inclination, $i$ ( $^\circ$ )	=	$10.8070 \pm 0.0014$
Longitude of the ascending node, $\Omega$ ( $^\circ$ )	=	$222.507 \pm 0.002$
Argument of perihelion, $\omega$ ( $^\circ$ )	=	$286.8 \pm 0.3$
Mean anomaly, $M$ ( $^\circ$ )	=	$271.2 \pm 0.6$
Perihelion, $q$ (au)	=	$15.73 \pm 0.03$
Aphelion, $Q$ (au)	=	$22.54 \pm 0.02$
Absolute magnitude, $H$ (mag)	=	9.7

the Canada–France–Hawaii Telescope (CFHT; Alexandersen et al. 2013a). The observations were made as part of an ongoing survey with CFHT, looking for trans-Neptunian objects (TNOs) and minor bodies located between the giant planets. However, they were not submitted to the Minor Planet Center (MPC) until March 2013 (the discovery was announced on 2013 March 18; Alexandersen et al. 2013a). The object was identified due to its relatively high proper motion with respect to the background stars. It is comparatively large with  $H = 9.7$  mag or a diameter close to 60 km assuming a 5 per cent albedo. Its orbit is now reasonably well determined with 29 observations spanning a data-arc of 419 d and it is characterized by  $a = 19.13$  au,  $e = 0.18$  and  $i = 10^\circ 81'$  (see Table 1). Using these orbital parameters, 2011 QF<sub>99</sub> has been classified as a Centaur by both the MPC Database<sup>3</sup> and the JPL Small-Body Database<sup>4</sup>. However, its period of revolution around the Sun, 83.69 yr at present, is very close to that of Uranus, 84.03 yr. That makes 2011 QF<sub>99</sub> a very good candidate to inhabit Uranus’ co-orbital region.

Asteroid 2011 QF<sub>99</sub> was identified as a Trojan of Uranus by Alexandersen et al. (2013b). It was the first Uranus’ Trojan observed and identified as such. Uranus’ Trojans share the semimajor axis of Uranus but they may have different eccentricity and inclination. In a frame of reference rotating with Uranus, they move in the so-called tadpole orbits around the Lagrangian equilateral points L<sub>4</sub> and L<sub>5</sub>; L<sub>4</sub> is located on the orbit of Uranus at some  $60^\circ$  ahead or east of Uranus, and L<sub>5</sub> is some  $60^\circ$  west. In other words, and for those objects, the relative mean longitude  $\lambda_r = \lambda - \lambda_{\text{Uranus}}$  oscillates around the values  $+60^\circ$  (L<sub>4</sub>) or  $-60^\circ$  (or  $+300^\circ$ , L<sub>5</sub>), where  $\lambda$  and  $\lambda_{\text{Uranus}}$  are the mean longitudes of the Trojan and Uranus, respectively. The mean longitude of an object is given by  $\lambda = M + \Omega + \omega$ , where  $M$  is the mean anomaly,  $\Omega$  is the longitude of the ascending node and  $\omega$  is the argument of perihelion. The two other main co-orbital states are quasi-satellite ( $\lambda_r$  oscillates around  $0^\circ$ ) and horseshoe ( $\lambda_r$  oscillates around the Lagrangian point L<sub>3</sub> which is located on the orbit of Uranus but at  $180^\circ$  from the planet) libration (see e.g. Mikkola et al. 2006; Murray & Dermott 1999, respectively, for further details). For any given planet-minor body pair,  $\lambda_r$  measures how far in orbital phase the minor body moves with respect to the planet. Under certain conditions, complex orbits, hybrid of two (or more) elementary resonant states, are also possible. For example, a compound orbit between the Trojan and quasi-satellite states is also called a large-amplitude Trojan when the libration amplitude is less than  $180^\circ$ . Such an orbit encloses L<sub>4</sub> (or L<sub>5</sub>) and Uranus it-

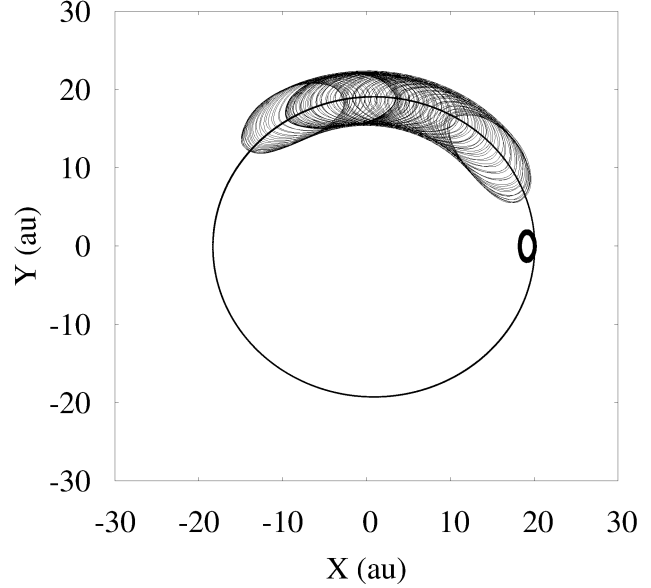


**Figure 1.** The motion of the asteroid 2011 QF<sub>99</sub> during the time interval  $(-5, 5)$  kyr projected on the ecliptic plane in a coordinate system rotating with Uranus. The orbit and the position of Uranus are also plotted. In this frame of reference, and as a result of its non-negligible eccentricity, Uranus describes a small ellipse. This figure is equivalent to fig. 1 in Alexandersen et al. (2013b).

self. Recurrent transitions between resonant states are possible for objects with both significant eccentricity and inclination (Namouni et al. 1999; Namouni & Murray 2000).

In Fig. 1, we plot the motion of 2011 QF<sub>99</sub> over the time range  $(-5, 5)$  kyr in a coordinate system rotating with Uranus. This figure is equivalent to fig. 1 in Alexandersen et al. (2013b). In this coordinate system, it appears to follow an oscillating oval-like path (the epicycle) around Uranus’ Lagrangian point L<sub>4</sub>. Its  $\lambda_r$  librates around  $+60^\circ$  with an amplitude close to  $100^\circ$ . We therefore confirm the current dynamical status of 2011 QF<sub>99</sub> as Trojan. Following the work of Mikkola et al. (2006), we define the relative deviation of the semimajor axis from that of Uranus by  $\alpha = (a - a_{\text{Uranus}})/a_{\text{Uranus}}$ , where  $a$  and  $a_{\text{Uranus}}$  are the semimajor axes of the object and Uranus, respectively. If we plot  $\alpha$  as a function of  $\lambda_r$  over the time range  $(-250, 250)$  kyr, we obtain Fig. 2 that further shows that the motion of 2011 QF<sub>99</sub> is confined and also that the mean oscillation centre is very close to  $+60^\circ$  in  $\lambda_r$ . For a Trojan, this object can stray relatively far from the Lagrangian point L<sub>4</sub> but it is not a large-amplitude Trojan because its orbit (in the rotating frame) does not currently enclose Uranus. It is not a horseshoe-Trojan libration hybrid either, because the object does not reach the Lagrangian point L<sub>3</sub>. This minor planet has remained in its present dynamical state for hundreds of thousands of years and it will continue to be trapped in this resonant configuration for some time into the future.

The current orbital behaviour of 2011 QF<sub>99</sub> is illustrated by the animation displayed in Fig. 3 (available on the electronic edition as a high-resolution animation). The orbit is presented in three frames of reference: Heliocentric (left), corotating with Uranus (top-right) and Uranocentric (bottom-right). The dynamical evolution of an object moving in a Trojan-like orbit associated with Uranus can be decomposed into a slow guiding centre librational motion and a superimposed short period three-dimensional

<sup>3</sup> [http://www.minorplanetcenter.net/db\\_search](http://www.minorplanetcenter.net/db_search)

<sup>4</sup> <http://ssd.jpl.nasa.gov/sbdb.cgi>

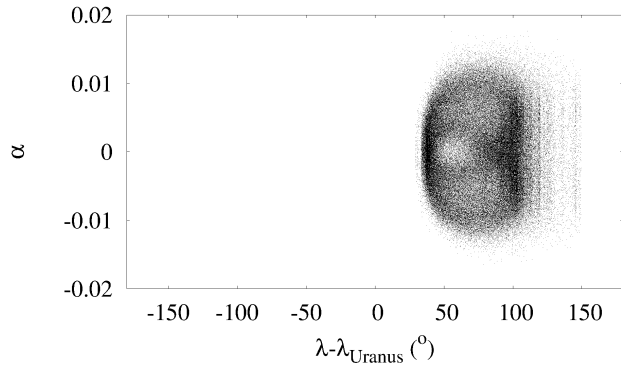


**Figure 2.** Resonant evolution of the asteroid 2011 QF<sub>99</sub> over the time range (-250, 250) kyr. The relative deviation of its semimajor axis from that of Uranus,  $\alpha$ , as a function of the relative mean longitude,  $\lambda_r$ , is displayed.

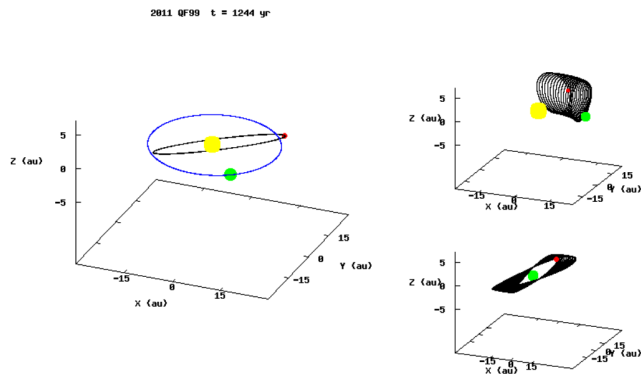


**Figure 3.** Three-dimensional evolution of the orbit of 2011 QF<sub>99</sub> in three different frames of reference: Heliocentric (left), frame corotating with Uranus but centred on the Sun (top-right), and Uranocentric (bottom-right). The red point represents 2011 QF<sub>99</sub>, the green one is Uranus, and the yellow one is the Sun. The osculating orbits are outlined and the viewing angle changes slowly to facilitate visualizing the orbital evolution. This figure is available on the electronic edition as a high-resolution animation.

epicyclic motion viewed in a frame of reference corotating with Uranus. The object spirals back and forth along Uranus' orbit and ahead of the planet with a period of nearly 5500 yr. This period changes slightly as a result of the changes in inclination. Each time the object gets close to Uranus, it is effectively repelled by the planet. In contrast, at the point of maximum separation from Uranus it is drawn towards the planet.

A plot of the evolution of the orbital elements of 2011 QF<sub>99</sub> over a 2 Myr interval centred on the present epoch is shown in Fig. 4. This figure displays the dynamical evolution of the nominal orbit (central panels) and those of two representative worst orbits which are most different from the nominal one. The orbit labelled as 'dynamically cold' (left-hand panels) has been obtained by subtracting three times the value of the respective uncertainty from the orbital parameters (the six elements) in Table 1. This orbit is the coldest, dynamically speaking, possible (lowest values of  $a$ ,  $e$  and  $i$ ) that is compatible with the current values of the orbital parameters of 2011 QF<sub>99</sub>. In contrast, the orbit labelled as 'dynamically hot' (right-hand panels) was computed by adding three times the value of the respective uncertainty to the orbital elements in Table 1. This makes this trajectory the hottest possible in dynamical terms (largest values of  $a$ ,  $e$  and  $i$ ).

All the control orbits exhibit consistent behaviour within a few dozen thousand years of  $t = 0$ . Dynamically colder orbits are less stable. The distance to 2011 QF<sub>99</sub> from Uranus is plotted in Fig. 4, panel A and shows that, in the future, the object undergoes close encounters with Uranus, near one Hill radius, prior to its departure from the co-orbital state. Such close encounters are also observed in the past, before its insertion in the co-orbital region. The evolution of  $\lambda_r$  in panel B indicates that, for the nominal orbit, the current co-orbital episode will end in about 0.37 Myr from now; then, 2011 QF<sub>99</sub> will decouple from Uranus with  $\lambda_r$  stopping its current libration and starting to circulate.

The nominal orbit displays a fairly stable evolution during the entire co-orbital episode; in contrast, the slightly different (but still compatible with the available observations) control orbits exhibit multiple transitions between the various co-orbital states. This is similar to what is observed in the case of 83982 Crantor (2002 GO<sub>9</sub>), a well studied Uranian horseshoe libration (de la Fuente Marcos & de la Fuente Marcos 2013b), even if this other object is far less stable (see below). Both L<sub>4</sub> and L<sub>5</sub> Trojan episodes are possible but horseshoe-like behaviour and even quasi-satellite episodes are also observed. The semimajor axis, panel C, exhibits the characteristic oscillatory behaviour associated with a 1:1 mean motion resonance. The value of the orbital eccentricity, panel D, stays under 0.2 for most of the co-orbital evolution and the inclination, panel E, remains confined to region B as defined in Dvorak et al. (2010). The argument of perihelion, panel F, mostly circulates, although some brief Kozai-like resonance (Kozai 1962) episodes are observed (see Fig. 4, F-panels).

All control calculations indicate that 2011 QF<sub>99</sub> has been co-orbital with Uranus for at least 0.5 Myr but less than 2 Myr. It will leave the co-orbital region in 50 kyr to 0.7 Myr from now. The most probable duration of the entire co-orbital episode is nearly 1 Myr. When trapped in the co-orbital region, its characteristic time-scale for chaotic divergence is  $\sim 10$  kyr. These results are consistent with those in Alexandersen et al. (2013b). In the following section we further investigate the details of the mechanism responsible for the insertion (ejection) of 2011 QF<sub>99</sub> into (from) the 1:1 mean motion resonance with Uranus.

#### 4 2011 QF<sub>99</sub>: STABILITY ANALYSIS

Asteroid 2011 QF<sub>99</sub> is currently confined to region B as defined in Dvorak et al. (2010), inclination interval (9, 13) $^\circ$ . Our numerical experiments indicate that, in this case, the instability surrounding this region is induced by the combined action of Jupiter and Neptune. Dvorak et al. (2010) argued that the instability at the high-inclination boundary ( $\sim 13^\circ$ ) is induced by Jupiter and Uranus but they could not identify the cause of instability at the low-inclination boundary ( $\sim 9^\circ$ ). Dvorak et al. (2010) integrations only include the Sun and the four gas giants. They studied the semimajor axis range 18.9–19.6 au with the orbital elements eccentricity, longitude of the node, and mean anomaly set to the corresponding values of Uranus ( $e_{\text{Uranus}} = 0.048$ ,  $\Omega_{\text{Uranus}} = 73^\circ.84$ ), and the argument of the perihelion  $\omega = \omega_{\text{Uranus}} \pm 60^\circ$  ( $\omega_{\text{Uranus}} = 95^\circ.74$ ). Some of these arbitrary choices have an impact on the applicability of their results to actual objects.

In any case, numerical integrations clearly indicate that the overall stability of individual Uranian co-orbitals not only depends on the orbital inclination but also on the eccentricity. Uranus horseshoe libration 83982 Crantor (2002 GO<sub>9</sub>) is also presently confined to region B (even if it is not currently a Trojan) but its eccentricity is

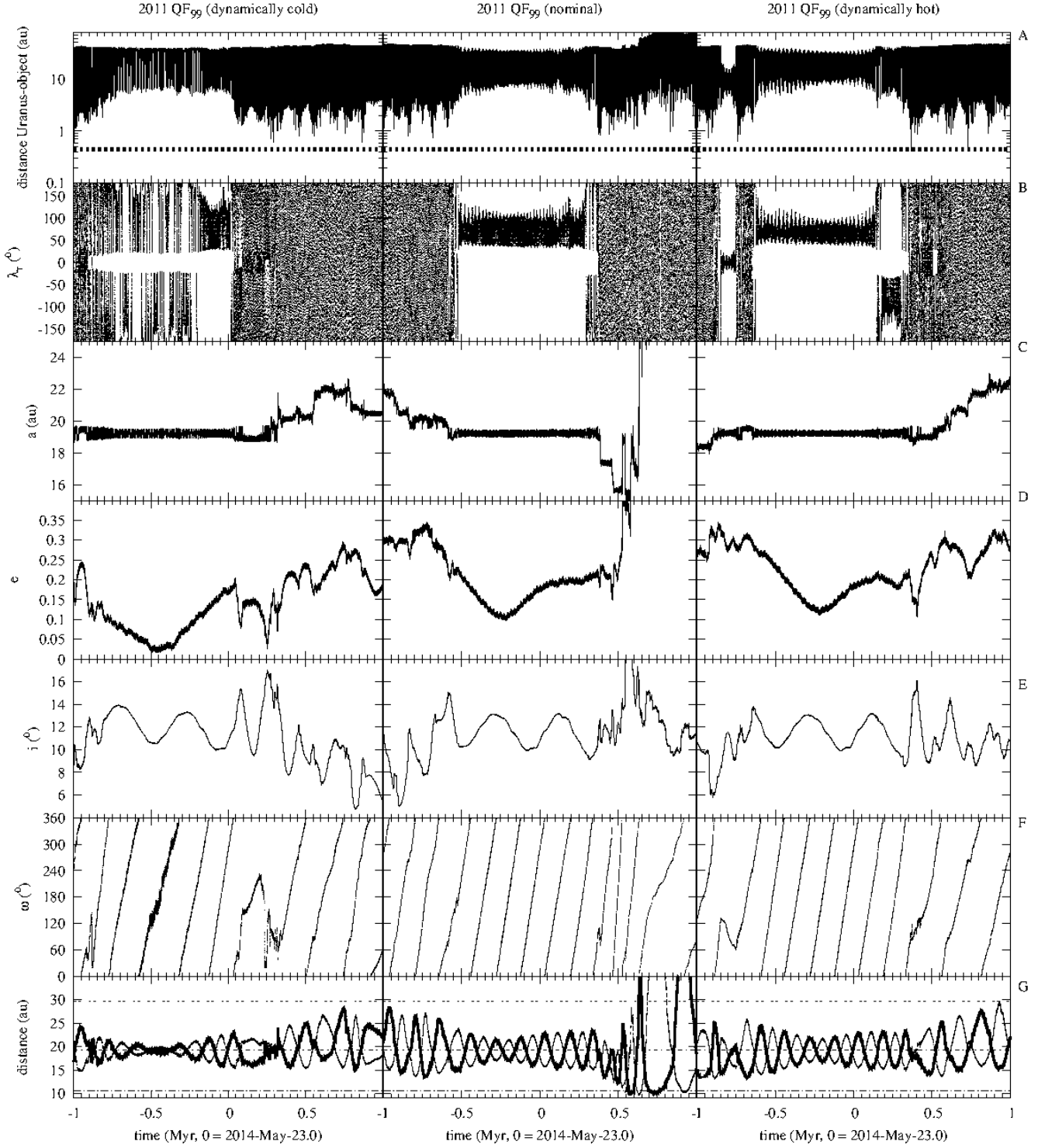


**Figure 4.** Time evolution of various parameters for the nominal orbit (central panels) and two representative examples of orbits that are most different from the nominal one in Table 1 (see the text for details). The distance of 2011 QF99 from Uranus (panel A); the value of the Hill sphere radius of Uranus, 0.447 au, is displayed. The resonant angle,  $\lambda_r$  (panel B). The orbital elements  $a$  (panel C) with the current value of Uranus' semimajor axis,  $e$  (panel D),  $i$  (panel E), and  $\omega$  (panel F). The distances to the descending (thick line) and ascending nodes (dotted line) are shown in the G-panels. Saturn's and Neptune's aphelion and perihelion distances as well as Uranus semimajor axis are also plotted. Fig. S1 in Alexandersen et al. (2013b) is partially equivalent to this figure.

higher ( $e = 0.27$ ) and, consistently, the destabilizing role of Saturn is enhanced with Neptune becoming a rather secondary perturber (de la Fuente Marcos & de la Fuente Marcos 2013b). The horseshoe libration candidate 2010 EU<sub>65</sub> is confined to a theoretically unstable region under Dvorak et al. (2010) analysis for Trojans ( $i = 14^\circ 84$ ) but its current dynamical status is significantly more stable than that of Crantor (or even 2011 QF<sub>99</sub>) due to its far lower eccentricity ( $e = 0.05$ ).

In its present orbit, 2011 QF<sub>99</sub> (and Uranus) moves in near resonance with the other three giant planets: 1:7 with Jupiter (period ratio of 0.142), 7:20 with Saturn (period ratio of 0.351) and 2:1 with Neptune (period ratio of 1.963). The dominant role played by Neptune and Jupiter on the orbital evolution of 2011 QF<sub>99</sub> must be connected with these near resonances and their possible superposition. Multibody resonances are a major source of chaos in the Solar system. In order to understand better what makes 2011 QF<sub>99</sub> (and other Uranian co-orbitals) dynamically unstable we study the time evolution of the resonant arguments  $\sigma_J = 7\lambda - \lambda_J - 6\varpi$ ,  $\sigma_S = 20\lambda - 7\lambda_S - 13\varpi$  and  $\sigma_N = \lambda - 2\lambda_N + \varpi$ , where  $\lambda_J$  is the mean longitude of Jupiter,  $\lambda_S$  is the mean longitude of Saturn,  $\lambda_N$  is the mean longitude of Neptune and  $\varpi = \Omega + \omega$  is the longitude of the perihelion of 2011 QF<sub>99</sub>. In Fig. 5, arguments  $\sigma_J$ ,  $\sigma_S$ ,  $\sigma_N$  and the relative mean longitude with respect to Uranus,  $\lambda_r$ , (thick line) are plotted against time for the interval (-25, 25) kyr. It is clear from the figure that present-day 2011 QF<sub>99</sub> is not in mean motion resonance with Jupiter or Neptune but it is trapped in the 7:20 mean motion resonance with Saturn. This finding is consistent with the analysis carried out by Gallardo (2006) in which he concluded that Uranus' Trojans are affected by high-order resonances with Saturn. The librations of both  $\sigma_S$  and  $\lambda_r$  are synchronized and  $\sigma_S$  alternates between circulation and asymmetric libration, indicating that the motion is chaotic. The argument  $\sigma_J$  exhibits a remarkable periodic behaviour but it does not librate; it may be very close to the separatrix in the phase space of the mean motion resonance though.

For the nominal orbit, the resonant behaviour displayed in Fig. 5 persists for about 0.7 Myr but it changes prior to the insertion of 2011 QF<sub>99</sub> into Uranus' co-orbital region and also before its ejection from the 1:1 commensurability (see below). For the control orbits, this resonant pattern is observed from 0.5 to over 2 Myr. As Trojan, 2011 QF<sub>99</sub> is submitted to a weak mean motion resonance with Saturn, characterized by an intermittent asymmetric libration, that is unable to terminate its co-orbital state. This is likely also the result of being very close to the separatrix in the phase space. In fact, this weak resonance with Saturn may make the tadpole orbit more stable. Even if 2011 QF<sub>99</sub> is not strictly submitted to any mean motion resonance with Jupiter or Neptune during its Trojan episode, their perturbations are strong enough to boost the libration amplitude of the tadpole path and likely contribute towards the long-term instability (chaotic diffusion) of the present resonant configuration.

Fig. 6 shows the evolution of the various resonant arguments for the nominal orbit just prior to the insertion of 2011 QF<sub>99</sub> into Uranus' co-orbital region. All the resonant arguments plotted were circulating 590 kyr before the current epoch. From the point of view of Uranus, the asteroid was a passing object. Then, a close encounter with Uranus sent 2011 QF<sub>99</sub> into the outskirts of Uranus' co-orbital region and into the 1:7 mean motion resonance with Jupiter and the 2:1 mean motion resonance with Neptune. The combined action of these two mean motion resonances, a three-body mean motion resonance (Nesvorný & Morbidelli 1998; Murray, Holman & Potter 1998), made 2011 QF<sub>99</sub> a horseshoe libration first and later an L<sub>4</sub> Trojan. For over 50 000 yr, the three-body reso-

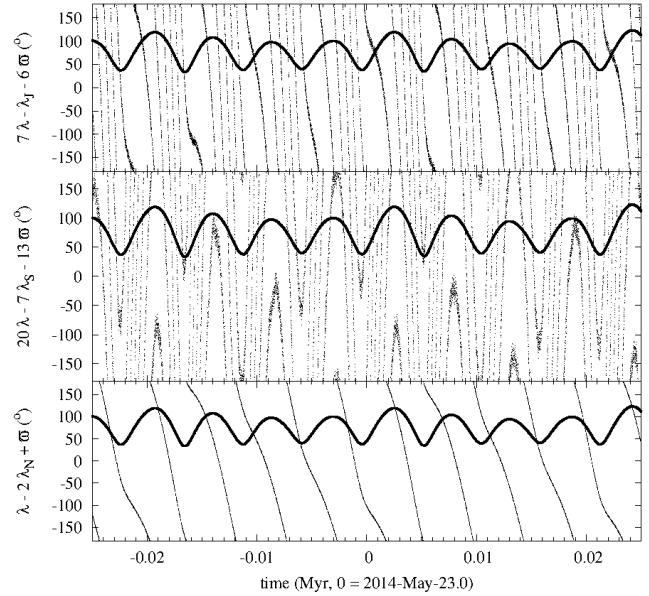


**Figure 5.** Asteroid 2011 QF<sub>99</sub>. Resonant arguments  $\sigma_J = 7\lambda - \lambda_J - 6\varpi$  (top panel),  $\sigma_S = 20\lambda - 7\lambda_S - 13\varpi$  (middle panel) and  $\sigma_N = \lambda - 2\lambda_N + \varpi$  (bottom panel) plotted against time for the time interval (-25, 25) kyr. The relative mean longitude with respect to Uranus appears as a thick line. The angle  $\sigma_S$  alternates between circulation and asymmetric libration, indicating that the motion is chaotic. The observed resonant evolution is consistent across control orbits.

nance was active, inserting the Centaur into a relatively stable configuration and also into the 7:20 mean motion resonance with Saturn. Capture into Uranus' co-orbital zone takes place at the low-inclination boundary ( $\sim 10^\circ$ ) of the stability island described by Dvorak et al. (2010). Nearly 545 kyr ago, 2011 QF<sub>99</sub> left the three-body resonance with Jupiter and Neptune and became firmly placed as Trojan. During the Trojan phase, 2011 QF<sub>99</sub> is also submitted to a three-body resonance, the 7:20 mean motion resonance with Saturn and the 1:1 mean motion resonance with Uranus. Remarkably, for the studied control orbits the sequence of events leading to Trojan capture is, in general, almost identical to the one described for the nominal orbit, only the timing is different.

The ejection from Uranus' co-orbital region follows a similar process. Fig. 7 shows the evolution of the same parameters plotted in Figs 5 and 6 for the nominal orbit before 2011 QF<sub>99</sub> becomes a passing object. The object was initially trapped in the 7:20 mean motion resonance with Saturn. Nearly 290 kyr into the future, the Trojan will fall again into the 1:7 mean motion resonance with Jupiter, leaving its tadpole orbit for an irregular horseshoe path. Nearly 80 kyr later, the object will leave the resonance with Jupiter, briefly entering the 2:1 mean motion resonance with Neptune. This perturbation effectively terminates the co-orbital episode with Uranus; the object becomes a passing Centaur again. Ejection from Uranus' co-orbital zone takes place at the high-inclination boundary ( $\sim 13^\circ$ ) of the stability island described by Dvorak et al. (2010). As in the case of capture, the dynamical evolution of the control orbits during ejection events is similar to the one described for the nominal orbit but with different timings. Our calculations clearly show that mean motion resonances with Jupiter and Neptune destabilize the co-orbital dynamics of 2011 QF<sub>99</sub>, eventually inducing close encounters with Uranus. This was first predicted by Marzari et al. (2003).

When studying isolated resonances, a critical angle is custom-

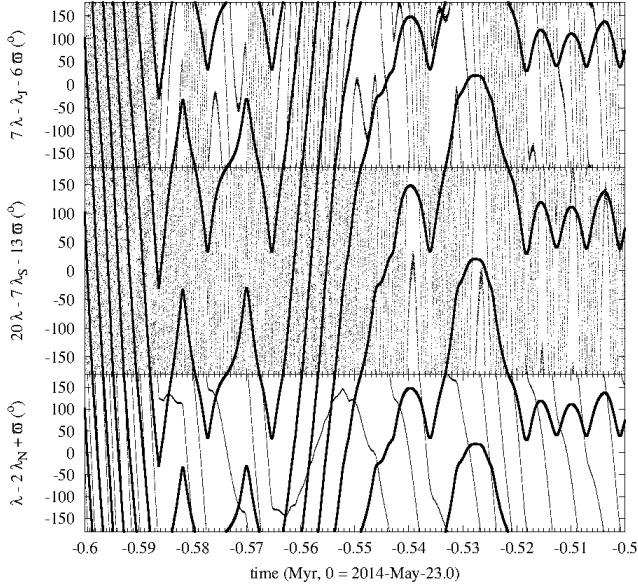


**Figure 6.** Asteroid 2011 QF<sub>99</sub>. Similar to Fig. 5 but for the time interval (-600, -500) kyr. The evolution of the various resonant arguments just prior to the insertion of 2011 QF<sub>99</sub> into Uranus’ co-orbital region is displayed.

arily defined so it exhibits different behaviour inside or outside the resonance, namely libration versus circulation. In contrast, our present study uncovers a resonant scenario characterized by highly nonlinear dynamics in which nested resonances are at work (see e.g. Morbidelli 2002). In addition, some of the resonances observed here are ephemeral, i.e. comparatively short-lived. Under such conditions, it is difficult to define a critical angle (see e.g. Robutel & Gabern 2006). This is why we focus on the natural candidates for low-order mean motion resonances, neglecting the possible existence of a, perhaps, better (and more complicated) critical angle relation that may be obtained by the means of an accurate determination of the proper frequencies. For additional details on this interesting issue, see Robutel & Gabern (2006).

It could be argued that, in co-orbital regime, it is difficult to distinguish between the 2:1 mean motion resonance with Neptune and a secondary resonance. Secondary resonances were introduced by Lemaître & Henrard (1990) and take place when there is a commensurability between apsidal and libration frequencies (for further details see Morbidelli 2002). Secondary resonances have been found for Jupiter’s Trojan asteroids (see Robutel & Gabern 2006). In our case, this is unlikely because the 2:1 resonance with Neptune is only observed for a few thousand years, during capture and ejection, not during the relatively long trapping inside the 1:1 mean motion resonance with Uranus. Secondary resonances may be present during the co-orbital phase as in the case of Jupiter’s Trojans but they probably have a very minor role for these transient objects.

In general, minor bodies that cross the paths of one or more planets can be rapidly destabilized by scattering resulting from close planetary approaches if their orbital inclinations are low. Asteroid 2011 QF<sub>99</sub> follows an eccentric orbit ( $e \approx 0.2$ ) but, currently, it only crosses the orbit of Uranus. This is also the case of Crantor and 2010 EU<sub>65</sub> (de la Fuente Marcos & de la Fuente Marcos 2013b), and like them, only close encounters with Uranus can activate or deactivate their co-orbital status with Uranus. All of them have similar, relatively significant orbital inclinations. In the Solar system, and for objects moving in inclined orbits, close

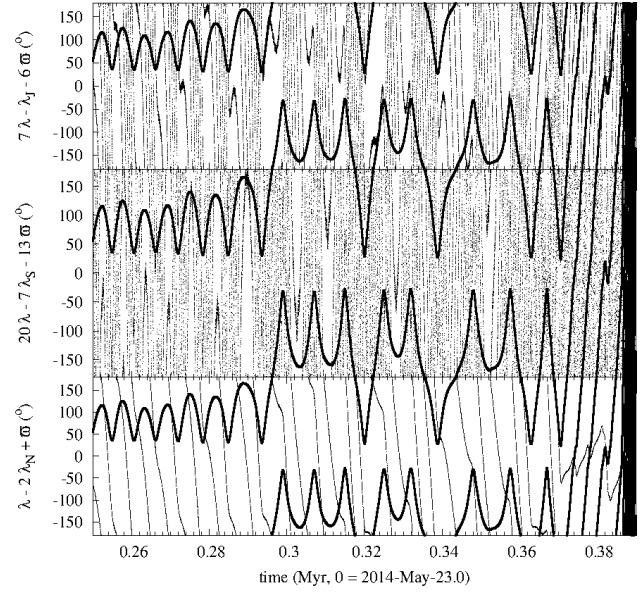


**Figure 7.** Asteroid 2011 QF<sub>99</sub>. Similar to Fig. 5 but for the time interval (250, 390) kyr. The evolution of the various resonant arguments before becoming a passing object.

encounters with major planets are only possible in the vicinity of the nodes. The distance between the Sun and the nodes is given by  $r = a(1 - e^2)/(1 \pm e \cos \omega)$ , where the ‘+’ sign denotes the ascending node and the ‘-’ sign the descending node.

Fig. 4, central G-panel shows the evolution of the distance to the nodes of 2011 QF<sub>99</sub> in the time range (-1, 1) Myr for the nominal orbit in Table 1. As in the case of Crantor and 2010 EU<sub>65</sub>, the evolution of the orbital elements in Fig. 4 shows that, for 2011 QF<sub>99</sub>, changes in  $\omega$  dominate those in  $a$  and  $e$  and largely control the positions of the nodes. The precession rate of the nodes is rather regular during co-orbital episodes but becomes chaotic when  $\lambda_r$  circulates. As pointed out below, this precession rate is somewhat synchronized with those of Jupiter and Uranus itself. Although the values of the nodal distances are currently very close to the value of the semimajor axis of Uranus, close (but relatively distant due to its Trojan status) flybys are only possible at the ascending node because the object is always east of Uranus when confined to the Trojan L<sub>4</sub> region. That makes it considerably more stable than Crantor, which experiences close encounters with Uranus at both nodes. For 2011 QF<sub>99</sub>, the combined action of Jupiter and Neptune drives the body out of the stable island and eventually completely out of the co-orbital region. This happens when  $\omega$  becomes 0° which also implies that its ascending node is now located at the perihelion distance i.e. the closest possible to Saturn and Jupiter. At that time, the descending node is found at the aphelion distance, the closest possible to Neptune. Under this arrangement, resonant perturbations are most effective as the perihelia of the various objects involved approximately lie along the same direction. Then, after ejection from the co-orbital region, close encounters with Saturn become possible as the nodal distances are able to reach Saturn’s aphelion (see Fig. 4, G-panels).

The behaviour pointed out above suggests that the precession frequency of the longitude of the perihelion of 2011 QF<sub>99</sub>,  $\varpi = \Omega + \omega$ , could be in secular resonance with one or more of the giant planets. There is a well-documented secular resonance between Uranus’ perihelion and Jupiter’s aphelion, as the difference



between the two librates around  $130^\circ$  within  $\sim \pm 70^\circ$  with a period of  $\sim 1.1$  Myr (Milani & Nobili 1985). This period is close to the most typical duration of the co-orbital episode of 2011 QF<sub>99</sub> with Uranus. Stockwell (1873) was first in realizing that the mean motion of Jupiter's perihelion is almost equal to that of Uranus, and that the mean longitudes of these perihelia differ by nearly  $180^\circ$ . Following e.g. Laskar (1990), the frequency that dominates the precession of both Jupiter's and Uranus' perihelia is  $g_5$ . If we represent the relative longitude of the perihelion,  $\Delta\varpi = \varpi - \varpi_P$ , where  $\varpi_P$  is the longitude of the perihelion of the studied planet, as a function of the time, we obtain Fig. 8. These plots show that only in the case of Saturn, the resonant argument  $\Delta\varpi$  circulates over the entire simulated time interval; the dominant frequency for Saturn's longitude of perihelion is  $g_6$  (see e.g. Laskar 1990). Before becoming a Uranian co-orbital both  $\varpi - \varpi_J$  and  $\varpi - \varpi_U$  circulated. After leaving the Trojan region,  $\varpi - \varpi_J$  starts to circulate again. As predicted by Marzari et al. (2003), during the Trojan episode the asteroid is in secular resonance with proper frequency  $g_5$ .

If  $\Delta\varpi = \varpi - \varpi_P$  librates around  $0^\circ$ , planet and object are very close to an stationary solution in which both orbits have their semimajor axes aligned so the conjunction occurs when planet and object are both at perihelion. If the libration is around  $180^\circ$ , then their perihelia lie in opposite directions. Fig. 8 shows that, for a relatively brief period of time, nearly 500 kyr ago,  $\varpi - \varpi_J$  librated symmetrically around  $0^\circ$ , when the object was also trapped in the 1:7 mean motion resonance with Jupiter. During this brief period of time, the two bodies were in apsidal corotation resonance (see Lee & Peale 2002; Beaugé, Ferraz-Mello & Michtchenko 2003) as their lines of apsides were aligned, maximizing the perturbation. Simultaneously,  $\varpi - \varpi_N$  librated around  $180^\circ$  meaning that, for a brief period of time, their perihelia lied on opposite directions. Prior to the ejection from the co-orbital region,  $\varpi - \varpi_U$  briefly librates around  $0^\circ$ . Having their lines of apsides aligned, the two objects encounter each other at perihelion and that sends 2011 QF<sub>99</sub> into the 1:7 mean motion resonance with Jupiter. Again an ephemeral double apsidal corotation is observed, symmetric with respect to Jupiter and anti-symmetric with respect to Neptune, and the object becomes a passing Centaur.

The region where the motion of 2011 QF<sub>99</sub> occurs during co-orbital insertion and ejection is part of a very chaotic domain where the superposition of mean motion and secular resonances severely complicates the dynamical study. Sometimes, the mean motion resonances are dense in phase space but, in some cases, they actually overlap. The ephemeral episodes of apsidal corotation observed between 2011 QF<sub>99</sub> and Jupiter corresponds to a Type I apsidal corotation as described in Beaugé et al. (2003).

## 5 TWO HORSESHOE LIBRATORS: 83982 CRANTOR (2002 GO<sub>9</sub>) AND 2010 EU<sub>65</sub>

Asteroid 83982 Crantor (2002 GO<sub>9</sub>) was initially proposed as Uranus' first co-orbital companion by Gallardo (2006). In his work, Crantor is identified as horseshoe liblator. Using an improved orbit, de la Fuente Marcos & de la Fuente Marcos (2013b) confirmed that Crantor is, in fact, a temporary horseshoe liblator. The short-term evolution of Crantor is displayed in Fig. 9 and it is substantially less stable than that of 2011 QF<sub>99</sub> in Fig. 4. Fig. 10 shows that the orbital evolution of this object is alternatively affected by the 1:7 mean motion resonance with Jupiter, the 7:20 with Saturn and the 2:1 with Neptune. At the present time, it is not actively submitted to any of these resonances but it was the combined action of the

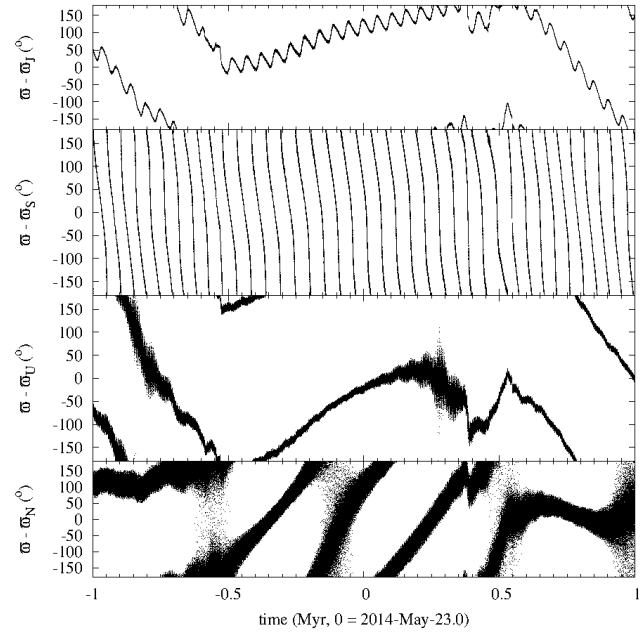


**Figure 8.** Time evolution of the relative longitude of the perihelion,  $\Delta\varpi$ , of 2011 QF<sub>99</sub> with respect to the giant planets: referred to Jupiter ( $\varpi - \varpi_J$ ), to Saturn ( $\varpi - \varpi_S$ ), to Uranus ( $\varpi - \varpi_U$ ) and to Neptune ( $\varpi - \varpi_N$ ). Only in the case of Saturn, the resonant argument  $\Delta\varpi$  circulates over the entire simulated period. These results are for the nominal orbit in Table 1.

1:7 mean motion resonance with Jupiter and the 2:1 mean motion resonance with Neptune, the one responsible for sending Crantor from the quasi-satellite to the horseshoe state nearly 6 kyr ago. The combination of resonances with Jupiter and Neptune will send the object back to the quasi-satellite state in about 7 kyr. During horseshoe libration episodes the relative mean longitude with respect to Uranus librates in synchrony with the resonant argument  $\sigma_S$ ; when Crantor is closest to Uranus,  $\sigma_S$  librates around  $180^\circ$ . Control orbits exhibit almost identical behaviour during horseshoe episodes (just slight difference in timings) but in most cases the 7:20 mean motion resonance with Saturn is also observed during the quasi-satellite phase. Differences observed between orbits starting with very similar initial conditions ( $< 1\sigma$  difference) are the result of chaos.

Objects moving in orbits similar to that of 2010 EU<sub>65</sub> are very stable Uranian co-orbitals, significantly more stable than 2011 QF<sub>99</sub>. All the control orbits indicate that this object may remain as a co-orbital companion to Uranus alternating the Trojan and horseshoe libration states for several ( $> 2$ ) Myr. If we study the resonant arguments  $\sigma_J$ ,  $\sigma_S$  and  $\sigma_N$  (see Figs 11 and 12), we observe that this object is also trapped in a mean motion resonance with Saturn during its co-orbital evolution as the other objects are at some point. The relative mean longitude with respect to Uranus librates in synchrony with the resonant argument  $\sigma_S$ . Both  $\sigma_J$  and  $\sigma_S$  alternate between circulation and asymmetric libration, indicating that the motion is chaotic. The argument  $\sigma_N$  mostly circulates but it must be very close to the separatrix. All the control orbits indicate that 2010 EU<sub>65</sub> is a relatively recent visitor probably from the Oort cloud. The object was likely captured in the 1:1 resonance with Uranus 1–3 Myr ago. If originated in the Oort cloud, it may have entered the Solar system nearly 3 Myr ago. It will remain as Uranus' co-orbital for 2–5 more Myr. After leaving Uranus' co-orbital region it could remain between the orbits of Uranus and



**Table 2.** Heliocentric Keplerian orbital elements (and the  $1\sigma$  uncertainty) of asteroids 1999 HD<sub>12</sub>, 83982 Crantor (2002 GO<sub>9</sub>), 2002 VG<sub>131</sub> and 2010 EU<sub>65</sub> (Epoch = JD2456800.5, 2014-May-23.0; J2000.0 ecliptic and equinox. Data for 1999 HD<sub>12</sub> are referred to epoch 2451300.5, 1999-May-02.0. Data for 2002 VG<sub>131</sub> are referred to epoch 2452601.5, 2002-Nov-23.0. Source: JPL Small-Body Database.)

		1999 HD <sub>12</sub>	(83982) Crantor	2002 VG <sub>131</sub>	2010 EU <sub>65</sub>
Semimajor axis, $a$ (au)	=	$19 \pm 32$	$19.3579 \pm 0.0014$	$19 \pm 12$	$19.3 \pm 0.3$
Eccentricity, $e$	=	$0.5 \pm 1.3$	$0.27603 \pm 0.00004$	$0.3 \pm 1.0$	$0.06 \pm 0.03$
Inclination, $i$ ( $^\circ$ )	=	$10.1 \pm 1.4$	$12.79126 \pm 0.00003$	$21 \pm 2$	$14.8 \pm 0.2$
Longitude of the ascending node, $\Omega$ ( $^\circ$ )	=	$178 \pm 2$	$117.4031 \pm 0.0003$	$213 \pm 2$	$4.583 \pm 0.011$
Argument of perihelion, $\omega$ ( $^\circ$ )	=	$291 \pm 46$	$92.437 \pm 0.003$	$100 \pm 98$	$192 \pm 70$
Mean anomaly, $M$ ( $^\circ$ )	=	$28 \pm 87$	$50.935 \pm 0.007$	$34 \pm 14$	$8 \pm 62$
Perihelion, $q$ (au)	=	$9 \pm 9$	$14.0146 \pm 0.0002$	$13 \pm 10$	$18.1 \pm 0.3$
Aphelion, $Q$ (au)	=	$29 \pm 48$	$24.701 \pm 0.002$	$26 \pm 17$	$20.5 \pm 0.3$
Absolute magnitude, $H$ (mag)	=	12.8	8.8	11.3	9.1

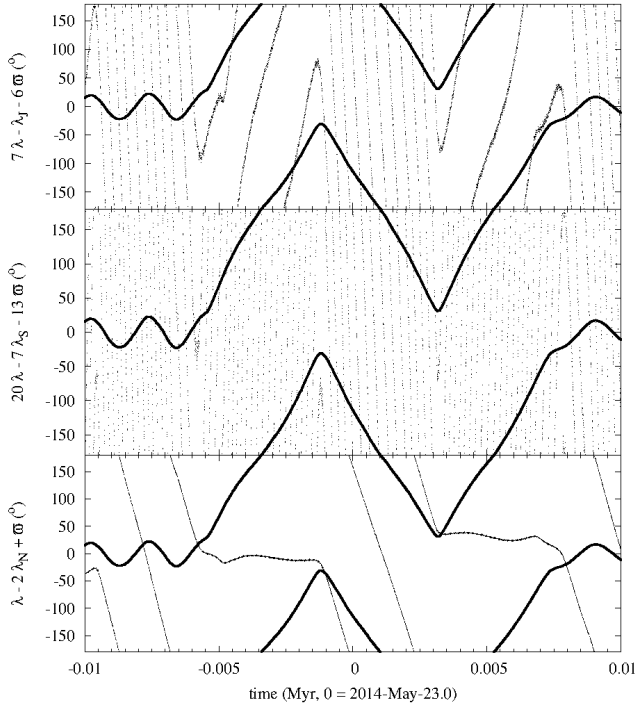


**Figure 10.** Asteroid 83982 Crantor (2002 GO<sub>9</sub>). Resonant arguments  $\sigma_J = 7\lambda - \lambda_J - 6\omega$  (top panel),  $\sigma_S = 20\lambda - 7\lambda_S - 13\omega$  (middle panel) and  $\sigma_N = \lambda - 2\lambda_N + \omega$  (bottom panel) plotted against time for the time interval (-10, 10) kyr. The relative mean longitude with respect to Uranus appears as a thick line. The resonant arguments exhibit alternating libration and circulation that trigger the transitions between the various co-orbital states.

Neptune for some time but it may also be ejected from the Solar system. Its co-orbital episode with Uranus will last for about 3–8 Myr.

## 6 URANIAN CO-ORBITALS: ARE THERE OTHERS?

Asteroid 2011 QF<sub>99</sub> was found during a survey mainly focused on TNOs. During the past 15 years or so, wide-field CCD surveys aimed at the outer Solar system have found dozens of objects moving in the neighbourhood of Uranus, many of which were classified using cuts in the perihelion,  $q$ , and other orbital parameters (as an

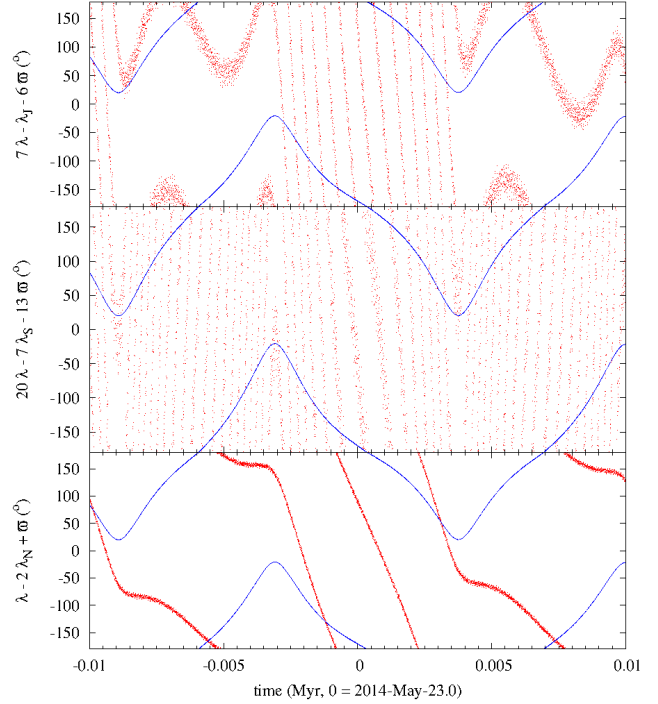


**Figure 11.** Asteroid 2010 EU<sub>65</sub>. Resonant arguments  $\sigma_J = 7\lambda - \lambda_J - 6\omega$  (top panel),  $\sigma_S = 20\lambda - 7\lambda_S - 13\omega$  (middle panel) and  $\sigma_N = \lambda - 2\lambda_N + \omega$  (bottom panel) plotted against time in red for the time interval (-10, 10) kyr. The relative mean longitude with respect to Uranus appears in blue. Both  $\sigma_J$  and  $\sigma_S$  alternate between circulation and asymmetric libration, indicating that the motion is chaotic but the resonant argument  $\sigma_S$  is synchronized with  $\lambda_r$ . The argument  $\sigma_N$  mostly circulates.

example, the MPC defines that Centaurs must have a perihelion larger than Jupiter’s orbit and a semimajor axis shorter than Neptune’s). This approach leads to misidentification of resonant minor bodies (Shankman 2012). Therefore, it is quite possible that some of these objects may have not been properly classified and that they may be trapped, perhaps just temporarily, in a 1:1 mean motion resonance with Uranus. Here, we explore this possibility and try to uncover additional Uranus’ co-orbitals. We select candidates with relative semimajor axis,  $|a - a_{\text{Uranus}}| \leq 0.15$  au, and use  $N$ -body simulations, as described above, to confirm or reject their current co-orbital nature with Uranus. Our selection criterion reveals two additional candidates: 1999 HD<sub>12</sub> and 2002 VG<sub>131</sub>. We call them

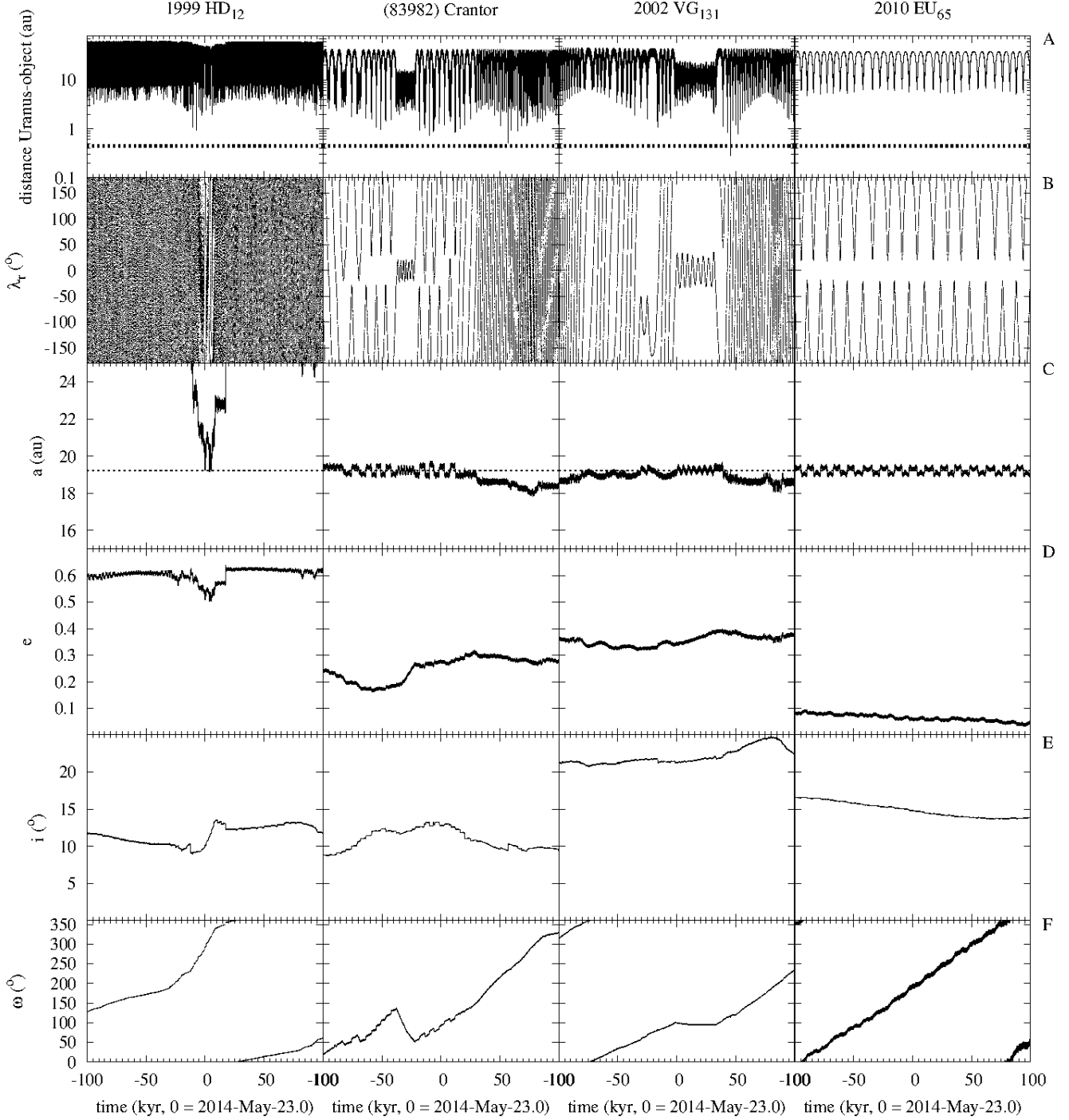


**Figure 9.** Time evolution of various parameters for the nominal orbits of known and new Uranian co-orbital candidates (see the text for details). The distance of the object from Uranus (panel A); the value of the Hill sphere radius of Uranus, 0.447 au, is displayed. The resonant angle,  $\lambda_T$  (panel B). The orbital elements  $a$  (panel C) with the current value of Uranus' semimajor axis,  $e$  (panel D),  $i$  (panel E), and  $\omega$  (panel F).

candidates because both objects have very short data-arcs. As a result, their orbits are very poorly determined. They are included here for completeness, to explore the dynamics of other possible short-term stable co-orbital parameter domains, and to encourage the acquisition of further observations to improve their orbital solutions.

Asteroid 1999 HD<sub>12</sub> was discovered on 1999 April 17 at  $R = 22.9$  mag by the Deep Ecliptic Survey (DES) observing with the 4 m Mayall Telescope at Kitt Peak National Observatory (Millis

et al. 1999; Bernstein & Khushalani 2000; Millis et al. 2002; Eliot et al. 2005). The uncertainties associated with its orbit are very large as it is based on just 11 observations with a data-arc of only 49 d. The orbital elements are:  $a = 19.34$  au,  $e = 0.52$ ,  $i = 10^\circ$ ,  $\Omega = 178^\circ$  and  $\omega = 291^\circ$ , with  $H = 12.8$  mag. Its orbital evolution is shown in Fig. 9 and it is extremely chaotic. If 83982 Crantor (2002 GO<sub>9</sub>) has an  $e$ -folding time of nearly 1 kyr, any object moving in an orbit similar to that of 1999 HD<sub>12</sub> has a much shorter

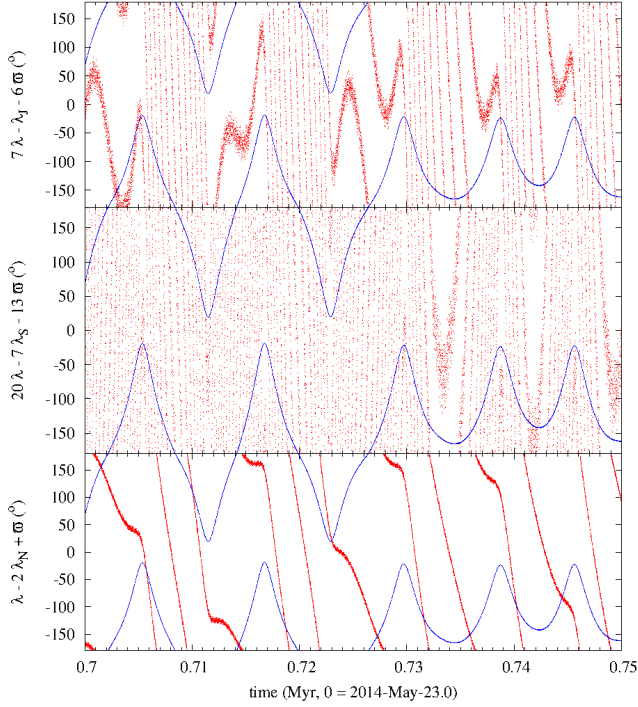


**Figure 12.** Same as Fig. 11 but for the time interval (0.70, 0.75) Myr.

$e$ -folding time ( $< 100$  yr). With a perihelion of 9.4 au and an aphelion of 29.3 au, close encounters with Saturn, Uranus and Neptune are possible. Its co-orbital episodes with Uranus are brief (a few kyr) and well scattered. Objects like this one may well signal the edge of Uranus' co-orbital region. Fig. 13 shows that it is submitted to a very complex set of mean motion resonances that involves all the giant planets. This explains the extremely chaotic behaviour observed (compare the evolution of  $\lambda_r$  for JD2456800.5 in Fig. 9 with that of JD2456600.5 in Fig. 13, for the same input observations).

Asteroid 2002 VG<sub>131</sub> was discovered on 2002 November 9 at  $R = 22.5$  mag also by DES (Meech et al. 2002; Elliot et al. 2005). Its orbit, based on six observations and spanning a data-arc of only 26 d, is very uncertain too. The orbital elements are:  $a = 19.10$  au,  $e = 0.34$ ,  $i = 21^\circ$ ,  $\Omega = 213^\circ$  and  $\omega = 100^\circ$ , with  $H = 11.2$  mag. It is currently a quasi-satellite, the first identified candidate in this resonant state for Uranus. The orbital evolution of 2002 VG<sub>131</sub> as depicted in Fig. 9 closely resembles that of Crantor, with a very similar  $e$ -folding time. It is very likely that most present-day, transient Uranian co-orbitals are dynamical analogues of Crantor and 2002 VG<sub>131</sub>. This object has been included by Jewitt (2009) in his study of active Centaurs with an effective radius of the nucleus of 11 km and a coma magnitude  $> 26.13$  mag (however, it was not active in 2002 December when it was observed by Keck). Regarding the influence of multibody resonances on the orbital evolution of this object, Fig. 14 shows that 2002 VG<sub>131</sub> is submitted to the same type of resonant evolution that affects Crantor.

## 7 DISCUSSION

The stability of the objects studied here reflects the chaos in the orbital evolution of the giant planets resulting from the superposition of three-body mean motion resonances for Jupiter, Saturn and Uranus as identified by Murray & Holman (2001). For large ob-

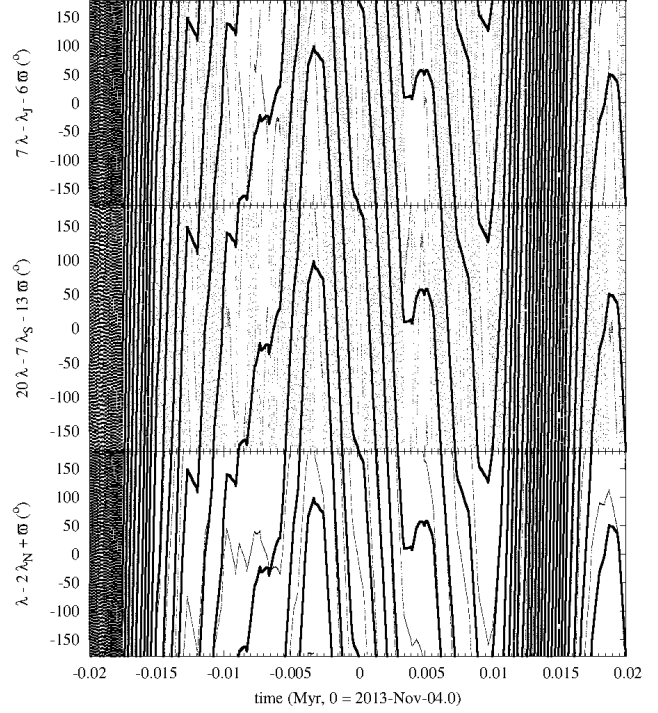


**Figure 13.** Asteroid 1999 HD<sub>12</sub>. Resonant arguments  $\sigma_J = 7\lambda - \lambda_J - 6\omega$  (top panel),  $\sigma_S = 20\lambda - 7\lambda_S - 13\omega$  (middle panel) and  $\sigma_N = \lambda - 2\lambda_N + \omega$  (bottom panel) plotted against time for the time interval (-20, 20) kyr. The relative mean longitude with respect to Uranus appears as a thick line. This object is submitted to a very complex set of mean motion resonances that involves all the giant planets.

jects, this translates into a chaotic but long-term stable system; for small bodies, this superposition turns out to be far from stable.

The dynamical evolution of the previously documented Uranus' co-orbital 83982 Crantor (2002 GO<sub>9</sub>) is very chaotic, the time-scale necessary for two initially infinitesimally close trajectories associated with this object to separate significantly, or  $e$ -folding time, is less than 1 kyr (de la Fuente Marcos & de la Fuente Marcos 2013b). In contrast, the characteristic  $e$ -folding time of 2011 QF<sub>99</sub> during the current Trojan episode has been found to be nearly 10 kyr. Therefore, simulations over long time-scales (e.g.  $\gg 1$  Myr) are not particularly useful in this case and we restrict our figures to just 2 Myr, maximum. Since the orbit of the asteroid is chaotic, its true phase-space trajectory will diverge exponentially from that obtained in our calculations. However, the evolution of most of the control orbits studied exhibit very similar secular behaviour of the orbital elements in the time interval (-100, 100) kyr. It is worth noting that, for most 2011 QF<sub>99</sub> control orbits, the close encounters with Uranus happen well beyond the ends of that interval. These encounters have the largest overall impact on the evolution of 2011 QF<sub>99</sub>. The predicted future evolution seems to be more consistent across control orbits than that of the past; i.e. the detailed dynamical evolution of this object is less predictable into the past even if it may have been more stable then. There is a wide dispersion regarding the actual time of insertion into Uranus' co-orbital region. The dynamical evolution of 2011 QF<sub>99</sub> as described by our integrations can be considered reliable within the time interval indicated above but beyond that, we regard our results as an indication of the probable dynamical behaviour of the minor body. However, the current dynamical status of the object is firmly established even

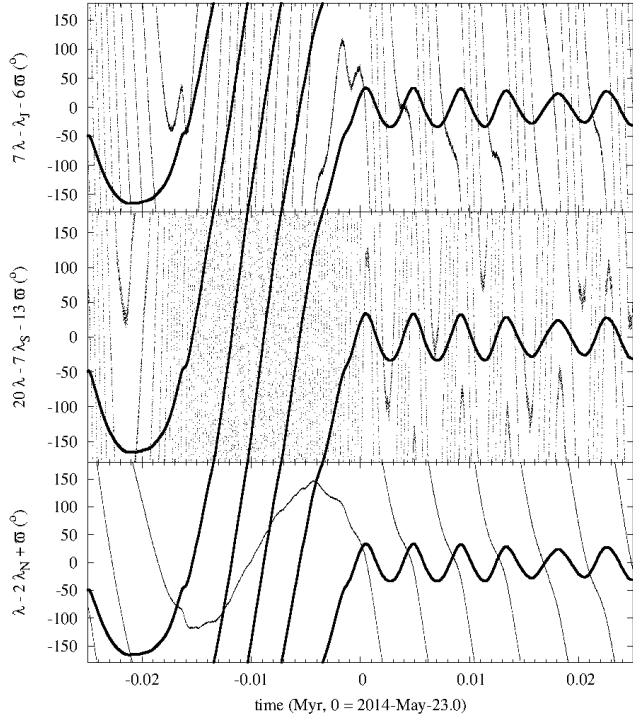


**Figure 14.** Asteroid 2002 VG<sub>131</sub>. Resonant arguments  $\sigma_J = 7\lambda - \lambda_J - 6\omega$  (top panel),  $\sigma_S = 20\lambda - 7\lambda_S - 13\omega$  (middle panel) and  $\sigma_N = \lambda - 2\lambda_N + \omega$  (bottom panel) plotted against time for the time interval (-25, 25) kyr. The relative mean longitude with respect to Uranus appears as a thick line. The resonant behaviour is very similar to that plotted in Fig. 10.

if the details of its dynamical evolution until it is ejected from the co-orbital region are affected by its inherently chaotic behaviour. Some control orbits only show Trojan behaviour with a very short horseshoe episode during insertion and just prior to ejection. More often, multiple transitions between the various co-orbital states are observed before ejection.

The comparative evolution of Uranus' co-orbital Crantor and candidates 1999 HD<sub>12</sub>, 2002 VG<sub>131</sub> and 2010 EU<sub>65</sub> is displayed in Fig. 9. It clearly shows that objects moving in 2010 EU<sub>65</sub>-like orbits are far more stable than any other currently known Uranus' co-orbital configuration, including that of 2011 QF<sub>99</sub>. This is the result of its low eccentricity. Unfortunately, 2010 EU<sub>65</sub> has not been reobserved since 2010 June. Hypothetical objects moving in low-eccentricity orbits and locked in a Kozai resonance (Kozai 1962) may be even more stable as in the case of the dynamically cold Kozai resonators described by Michel & Thomas (1996) or de la Fuente Marcos & de la Fuente Marcos (2013a). These have not been found yet in the case of Uranus but they may exist at other inclinations. The orbital evolutions of Crantor and 2002 VG<sub>131</sub> are remarkably similar and they briefly exhibit Kozai-like dynamics, the argument of the perihelion librates (or remains almost constant) around 90° (see Fig. 9, panel F, second and third columns). 2002 VG<sub>131</sub> has not been reobserved since 2002 December. Both 2002 VG<sub>131</sub> and 2010 EU<sub>65</sub> are very interesting targets for recovery; their short-term stability should make that task easier. In sharp contrast, the paths of objects moving in 1999 HD<sub>12</sub>-like orbits are so chaotic that the prospects of recovery for this object are rather slim; its last observation was recorded almost 15 years ago and this time-span is practically of the same order as its  $e$ -folding time.

The destabilizing role of the 1:7 mean motion resonance with

Jupiter in the case of Uranus' co-orbitals is just another example of how asymmetric libration in the region exterior to a perturbing mass is intrinsically more chaotic than that in the interior region. Winter & Murray (1997) studied the stability of asymmetric periodic orbits associated with the 1: $n$  resonances and how chaos is induced at these resonances: hardly any actual asteroids are trapped in exterior 1: $n$  resonances in the Solar system. The role of the exterior resonance with Jupiter on the dynamics of 2011 QF<sub>99</sub> cannot be neglected, nor can we ignore its influence on the dynamics of other Uranian co-orbitals. As for secular resonances, if we represent the relative longitude of the perihelion,  $\Delta\varpi$ , for all these objects, as we did for 2011 QF<sub>99</sub>, we obtain Fig. 15. Consistently with the case of 2011 QF<sub>99</sub>, the resonant argument circulates only for Saturn. With the exception of 2010 EU<sub>65</sub>, the overall behaviour is similar to the one observed and discussed for 2011 QF<sub>99</sub>.

Of the 257 asteroids and 165 comets with semimajor axis in the range (6, 34) au currently in the MPC Database, five asteroids have been identified as temporary Uranian co-orbitals (or candidates). Comet C/1942EA (Väisälä 2) is also a candidate to be a temporary Uranian co-orbital. It means that nearly 2 per cent of the known asteroids with semimajor axis in that range are Uranian co-orbitals. According to Alexandersen et al. (2013b), the intrinsic fraction should be 0.4 per cent with less than a factor of 2 variation. The current tally already appears to be five times larger than their theoretical expectations and this suggests that our current understanding of the origin and dynamics of this resonant population may not be complete. Discrepancies may have their origin in collisional processes. Three objects (Crantor, 2010 EU<sub>65</sub> and 2011 QF<sub>99</sub>) have absolute magnitude  $< 10$ , the others have  $> 11$  mag. Using the results of collisional evolution calculations, Fraser (2009) has predicted the existence of a break in the size distribution (therefore, also in the absolute magnitude distribution) of TNOs somewhere in the 10–100 km range. Asteroids 1999 HD<sub>12</sub> and 2002 VG<sub>131</sub> may be fragments of larger objects, the result of collisional evolution.

Predictions from simulations (see Section 1) appear to suggest that additional Uranus' transient co-orbitals should exist, although recent modelling by Alexandersen et al. (2013b) indicates that the current fraction is consistent with expectations. However, this appears to be in fact at odds with the observational evidence if all five co-orbitals and candidates are considered. On the other hand, additional temporary (yet to be detected) co-orbitals may be in the form of intrinsically fainter objects (apparent magnitude at perigee  $> 23$  mag, see Table 3), the result of collisional processes. If this hypothesis is correct, where can they be preferentially found if their orbital elements are similar to those of the already identified co-orbitals and candidates? We try to answer this question in the following section.

## 8 HUNTING FOR URANIAN CO-ORBITALS: A PRACTICAL GUIDE

So far, the information collected from the various co-orbitals and candidates appears fragmentary, disparate and not particularly useful to search for additional Uranus' co-orbitals. However, we already know a few robust facts about their orbits: i) their relative (to Uranus) semimajor axes are likely  $\leq 0.15$  au, ii) their eccentricities are probably  $\leq 0.5$ , and iii) there are perhaps certain islands of stability in inclination. On the other hand, and in order to maximize the chances of discovery, we know that objects must be observed near perigee (that is sometimes but not always near perihelion due

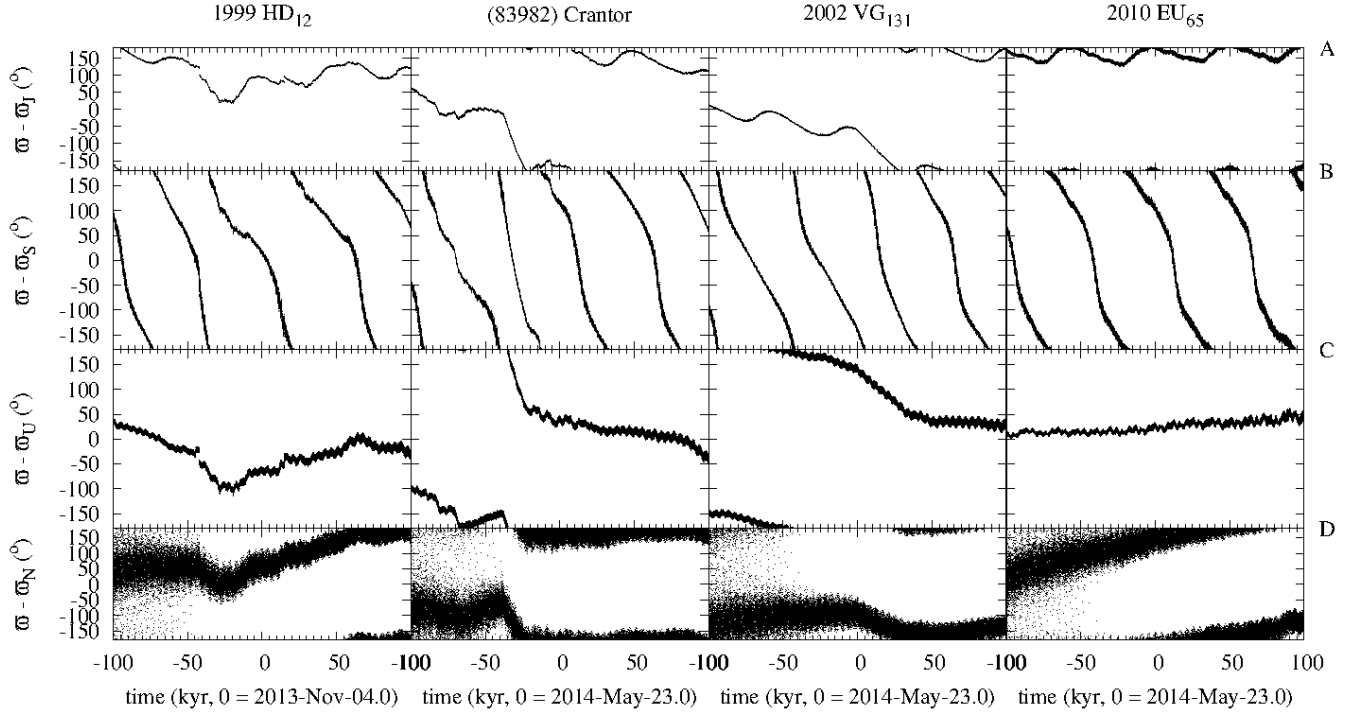


**Figure 15.** Time evolution of the relative longitude of the perihelion,  $\Delta\omega$ , of 1999 HD<sub>12</sub>, 83982 Crantor (2002 GO<sub>9</sub>), 2002 VG<sub>131</sub> and 2010 EU<sub>65</sub>. This figure is analogue to Fig. 8. Only in the case of Saturn, the resonant argument circulates.

to the relative geometry of the orbits). The condition of being located at relatively small angular separations from Uranus is only true for quasi-satellites. It is clear from our previous calculations that, in general, any angular separation from Uranus is possible, particularly for horseshoe librators. Transient Uranus' co-orbitals easily switch between resonant states and they can change from Trojan to horseshoe libration on a time-scale of kyr. If they must be found near perigee, when their apparent magnitude is the lowest because their distance from the Earth is the shortest, the Solar elongation becomes a non-issue as it will always be  $> 100^\circ$ .

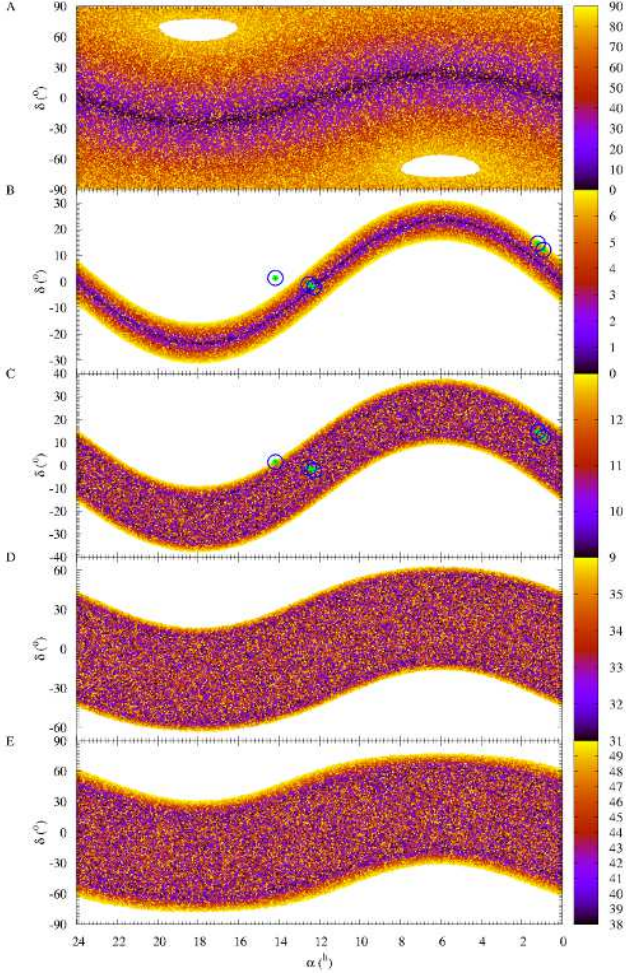
We have put all these ingredients at work in a Monte Carlo-type simulation, using the optimal ranges for semimajor axis, eccentricity and inclination, and assuming that  $\Omega$  and  $\omega \in (0, 360)^\circ$ , to compute the geocentric equatorial coordinates ( $\alpha$ ,  $\delta$ ) of hypothetical objects moving in Uranus' co-orbital candidate orbits when they are closest to the Earth (i.e. when their apparent magnitudes are the lowest). A uniform distribution is used to generate the orbital elements because the actual distribution in orbital parameter space is unknown. We do not assume any specific size (absolute magnitude) distribution as we are not trying to calculate any detection efficiency. However, any Uranian co-orbitals resulting from collisional evolution (i.e. objects like 1999 HD<sub>12</sub> or 2002 VG<sub>131</sub>) with sizes below  $\sim 10$  km (or absolute magnitude  $> 10$  mag) reach perigee with apparent magnitude  $> 22$ – $23$ .

Fig. 16 summarizes our findings in terms of location on the sky in equatorial coordinates at perigee as seen from the centre of the Earth for  $i \in (0, 90)^\circ$  (panel A) and the islands of stability (panels B, C, D and E) in Dvorak et al. (2010). In this, and in Fig. 17, the value of the parameter in the appropriate units is colour coded following the scale printed on the associated colour box (grey-scale in the printed version of the journal). Fig. 17 presents our results in terms of the perigee and the orbital elements. The equatorial coordinates at the time of discovery of the five objects discussed in

this paper are displayed in Fig. 16, panels B and C. Out of five discoveries, four of them appear in two pairs projected towards the same two areas of sky (see Table 3). The fifth one is 83982 Crantor (2002 GO<sub>9</sub>) itself that was serendipitously found by the Near-Earth Asteroid Tracking (NEAT) program on 2002 April 12 at Palomar Observatory. The NEAT program was not designed to target minor bodies in the outer Solar system.

Statistically speaking, and assuming uniformly distributed orbital elements within the ranges pointed out above, the best areas to search for these objects are located around right ascension  $0^h$  and  $12^h$  and declination  $\in (-20, 20)^\circ$  (see Fig. 18). Hypothetical high-inclination, high-eccentricity objects are expected to be discovered at higher declinations. The frequency variation between observing at  $6^h$  or  $18^h$  and observing at  $0^h$  or  $12^h$  is higher than 20 per cent, so statistically significant. Four out of five objects have been discovered at right ascensions near the statistically optimal values of  $0^h$  and  $12^h$ . On the other hand, the shortest perigees are preferentially found towards the ecliptic poles (see Fig. 17, top panel); the easiest to spot objects, if they do exist, have perigees well away from the ecliptic plane and they move in near polar orbits. In principle, these hypothetical objects may be unstable Kozai; but they could be submitted to the nodal libration mechanism (see Verrier & Evans 2008, 2009; Farago & Laskar 2010) and that may make them long-term stable. It is obvious that a significant fraction of the celestial sphere has not yet been surveyed for Uranian co-orbitals and that the scarcity pointed out in Section 1 may not only be due to strong perturbations by the other giant planets but also the result of observational bias. The most numerous objects may be the ones with absolute magnitude  $\sim 14$  mag (diameter  $\sim 1$  km, Fraser 2009) and they reach perigee with apparent magnitudes 24–25.





**Figure 16.** Distribution in equatorial coordinates of Uranus’ co-orbital candidate orbits at perigee as a function of the inclination (regions as defined in Dvorak et al. 2010). Full set of prograde orbits (panel A); region A (panel B); region B (panel C); region C (panel D); region D (panel E). The results for several millions of test orbits are displayed. The green points in panels B and C represent the discovery coordinates of the five objects discussed in this paper (see actual data in Table 3). The darkest lane outlines the ecliptic.

**Table 3.** Equatorial coordinates and apparent magnitudes (with filter) at discovery time for the five objects discussed in this paper. (J2000.0 ecliptic and equinox. Source: MPC Database.)

Object	$\alpha$ (h:m:s)	$\delta$ (°:′:″)	$m$ (mag)
1999 HD <sub>12</sub>	12:31:54.80	-01:03:07.9	22.9 (R)
(83982) Crantor	14:10:43.80	+01:24:45.5	19.2 (R)
2002 VG <sub>131</sub>	00:54:57.98	+12:07:52.4	22.5 (R)
2010 EU <sub>65</sub>	12:15:58.608	-02:07:16.66	21.2 (R)
2011 QF <sub>99</sub>	01:57:34.729	+14:35:44.64	22.8 (r)

## 9 CONCLUSIONS

In this paper, we have presented a detailed analysis of the orbital evolution and stability of present-day Uranus’ co-orbitals, focusing on how they got captured in the first place and what makes them dynamically unstable. Our calculations show that these objects are submitted to multiple mean motion resonances and exhibit signif-

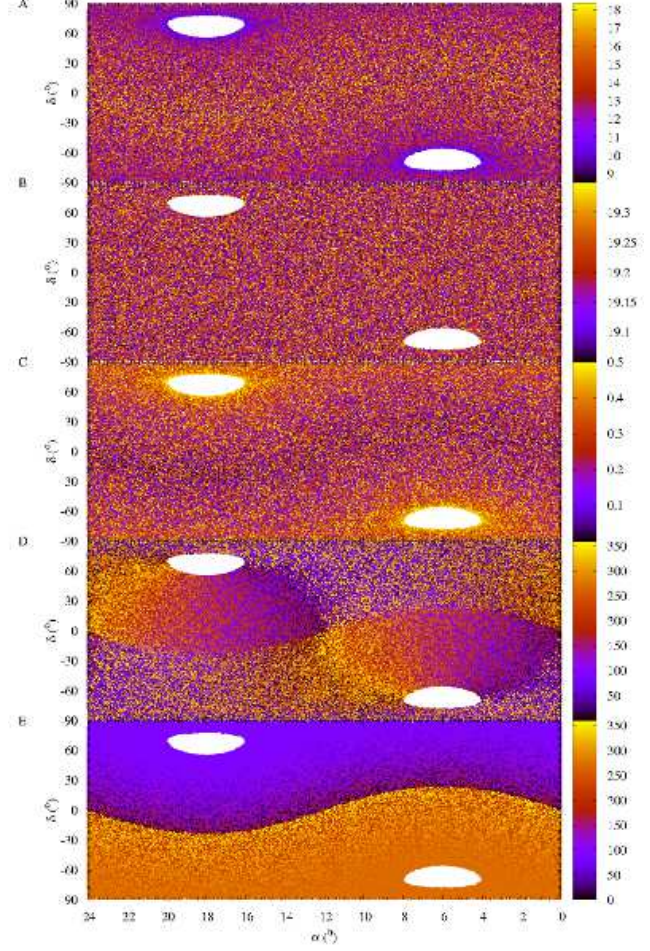


**Figure 17.** Distribution in equatorial coordinates of Uranus’ co-orbital candidate orbits at perigee as a function of various orbital elements and parameters. As a function of the perigee of the candidate (panel A); as a function of  $a$  (panel B); as a function of  $e$  (panel C); as a function of  $\Omega$  (panel D); as a function of  $\omega$  (panel E).

icant secular dynamics characterized by a complex structure that sometimes includes apsidal corotations. The dynamical behaviour analysed here is a typical example of highly nonlinear dynamics, resonances inside a resonance or even resonances inside a resonance. This is best studied using numerical simulations not analytical or semi-analytical work. Some of our results verify predictions made by Marzari et al. (2003) after studying the diffusion rate of Uranian Trojans.

We confirm that 2011 QF<sub>99</sub> currently moves inside Uranus’ co-orbital region on a tadpole orbit. The motion of this object is primarily driven by the influence of the Sun and Uranus, although both Jupiter and Neptune play a significant role in destabilizing its orbit. The resonant influence of Jupiter and Neptune was determinant in its capture as Uranus’ co-orbital. The precession of the nodes of 2011 QF<sub>99</sub>, which appears to be controlled by the combined action of Saturn and Jupiter, marks its evolution and short-term stability. A three-body mean motion resonance is responsible for both its injection into Uranus’ co-orbital region and its ejection from that region. The object will remain as Uranus Trojan for (very likely) less than 1 Myr. Even if 2011 QF<sub>99</sub> is one of the most stable of the known bodies currently trapped in the 1:1 commensurability with Uranus, it is unlikely to be a primordial 1:1 liberator.

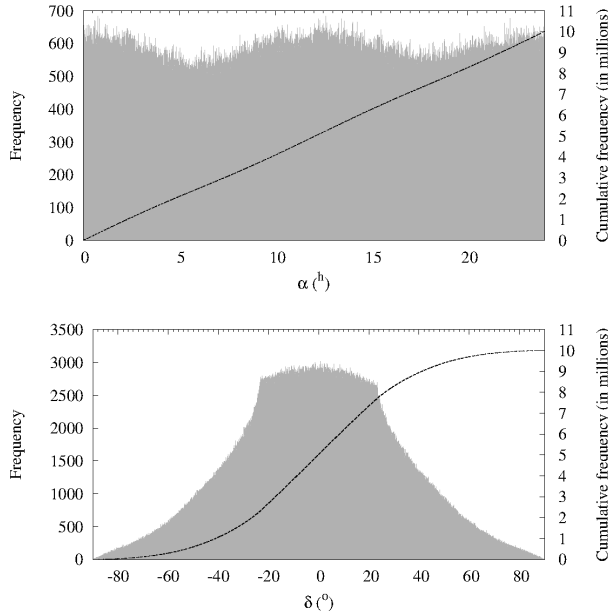


**Figure 18.** Frequency distribution in equatorial coordinates (right ascension, top panel, and declination, bottom panel) of Uranus' co-orbital candidate orbits at perigee. The best areas to search for these objects are located around right ascension  $0^h$  and  $12^h$  and declination  $\in (-20, 20)^\circ$ .

Our comparative study of currently known Uranus' co-orbitals and candidates shows that the candidate 2010 EU<sub>65</sub> is more stable than 2011 QF<sub>99</sub> because of its lower eccentricity (0.05 versus 0.18) even if 2010 EU<sub>65</sub> has higher orbital inclination ( $14^\circ.8$  versus  $10^\circ.80$ ). On the other hand, a new candidate, 2002 VG<sub>131</sub>, is found to exhibit dynamical behaviour very similar to the one discussed for 83982 Crantor (2002 GO<sub>9</sub>) in de la Fuente Marcos & de la Fuente Marcos (2013b) and here. This new candidate is the first identified quasi-satellite of Uranus; Crantor will also become a quasi-satellite in the near future. The presence of two objects characterized by similar dynamics and found by chance suggests that others, yet to be discovered, may share their properties. Asteroid 1999 HD<sub>12</sub> may signal the edge of Uranus' co-orbital region. In any case, all these objects have present-day dynamical ages much shorter than that of the Solar system; therefore, they are not members of a hypothetical population of primordial objects trapped in a 1:1 mean motion resonance with Uranus since the formation of the Solar system. They may be former primordial Neptune co-orbitals (Horner & Lykawka 2010) though.

Horner & Evans (2006) argued that present-day Uranus cannot efficiently trap objects in the 1:1 commensurability even for short periods of time. However, the available evidence confirms that, contrary to this view and in spite of the destabilizing role of the other giant planets, Uranus still can actively capture temporary co-orbitals, even for millions of years. Regarding the issue of stability, both Crantor's and 2011 QF<sub>99</sub>'s orbital inclinations are within one of the stability islands identified by Dvorak et al. (2010) for the case of Trojans. Both candidates 2002 VG<sub>131</sub> and 2010 EU<sub>65</sub> move outside the stability islands proposed in that study although they are not Trojans. The existence of 1999 HD<sub>12</sub> shows that not only inclination but also eccentricity play an important role in the long-term stability of Uranus' co-orbitals. A larger sample of Uranus' co-orbitals is necessary to understand better the complex subject of the stability of these objects although temporary Uranian co-

orbitals are often submitted to complicated multibody ephemeral mean motion resonances that trigger the switching between the various resonant co-orbital states, making them dynamically unstable.

Currently available evidence suggests that the small number of known transient Uranus' co-orbitals may have its origin in observational bias rather than in the strength of the gravitational perturbations by the other giant planets. Taking this into account, the number of yet undiscovered transient Uranian co-orbitals may likely be as high as that of the Neptunian ones. Our results can easily be applied to implement improved strategies for discovering additional Uranian co-orbitals.

## ACKNOWLEDGEMENTS

We would like to thank the anonymous referee for his/her quick and to-the-point reports, and to S. J. Aarseth for providing one of the codes used in this research. This work was partially supported by the Spanish 'Comunidad de Madrid' under grant CAM S2009/ESP-1496. We thank M. J. Fernández-Figueroa, M. Rego Fernández and the Department of Astrophysics of the Universidad Complutense de Madrid (UCM) for providing computing facilities. Most of the calculations and part of the data analysis were completed on the 'Servidor Central de Cálculo' of the UCM and we thank S. Cano Alsúa for his help during this stage. In preparation of this paper, we made use of the NASA Astrophysics Data System, the ASTRO-PH e-print server and the MPC data server.

## REFERENCES

- Aarseth S. J., 2003, *Gravitational N-body simulations*. Cambridge Univ. Press, Cambridge, p. 27
- Alexandersen M., Kavelaars J., Petit J., Gladman B., 2013a, *MPEC Circ.*, MPEC 2013-F19
- Alexandersen M., Gladman B., Greenstreet S., Kavelaars J. J., Petit J.-M., Gwyn S., 2013b, *Science*, 341, 994
- Beaugé C., Ferraz-Mello S., Michtchenko T. A., 2003, *ApJ*, 593, 1124
- Bernstein G., Khushalani B., 2000, *AJ*, 120, 3323
- de la Fuente Marcos C., de la Fuente Marcos R., 2012a, *MNRAS*, 427, 728
- de la Fuente Marcos C., de la Fuente Marcos R., 2012b, *A&A*, 545, L9
- de la Fuente Marcos C., de la Fuente Marcos R., 2012c, *A&A*, 547, L2
- de la Fuente Marcos C., de la Fuente Marcos R., 2013a, *MNRAS*, 434, L1
- de la Fuente Marcos C., de la Fuente Marcos R., 2013b, *A&A*, 551, A114
- Dvorak R., Bazsó Á., Zhou L.-Y., 2010, *Celest. Mech. Dyn. Astron.*, 107, 51
- Elliot J. L. et al., 2005, *AJ*, 129, 1117
- Farago F., Laskar J., 2010, *MNRAS*, 401, 1189
- Fraser W. C., 2009, *ApJ*, 706, 119
- Gacka I., 2003, *Ap&SS*, 284, 1069
- Gallardo T., 2006, *Icarus*, 184, 29
- Gallardo T., 2014, *Icarus*, 231, 273
- Giorgini J. D. et al., 1996, *BAAS*, 28, 1158
- Gomes R. S., 1998, *AJ*, 116, 2590
- Grav T. et al., 2011, *ApJ*, 742, 40
- Holman M. J., Wisdom J., 1993, *AJ*, 2015, 1987
- Horner J., Evans N. W., 2006, *MNRAS*, 367, L20
- Horner J., Lykawka P. S., 2010, *MNRAS*, 402, 13
- Innanen K. A., Mikkola S., 1989, *AJ*, 97, 900
- Jewitt D. C., 2009, *AJ*, 137, 4296
- Jewitt D. C., Trujillo C. A., Luu J. X., 2000, *AJ*, 120, 1140
- Kortenkamp S. S., Malhotra R., Michtchenko T., 2004, *Icarus*, 167, 347
- Kozai Y., 1962, *AJ*, 67, 591
- Laskar J., 1990, *Icarus*, 88, 266
- Lee M. H., Peale S. J., 2002, *ApJ*, 567, 596



- Lemaître A., Henrard J., 1990, *Icarus*, 83, 391
- Lykawka P. S., Horner J., 2010, *MNRAS*, 405, 1375
- Makino J., 1991, *ApJ*, 369, 200
- Marzari F., Tricarico P., Scholl H., 2003, *A&A*, 410, 725
- Masaki Y., Kinoshita H., 2003, *A&A*, 403, 769
- Meech K. J. et al., 2002, *MPEC Circ.*, MPEC 2002-X26
- Michel P., Thomas F., 1996, *A&A*, 307, 310
- Mikkola S., Innanen K., 1992, *AJ*, 104, 1641
- Mikkola S., Innanen K., Wiegert P., Connors M., Brasser R., 2006, *MNRAS*, 369, 15
- Milani A., 1993, *Celest. Mech. Dyn. Astron.*, 57, 59
- Milani A., Nobili A. M., 1985, *Celest. Mech.*, 35, 269
- Millis R. L. et al., 1999, *MPEC Circ.*, MPEC 1999-K18
- Millis R. L., Buie M. W., Wasserman L. H., Elliot J. L., Kern S. D., Wagner R. M., 2002, *AJ*, 123, 2083
- Morbidelli A., 2002, *Modern Celestial Mechanics: Aspects of Solar System Dynamics*. Taylor & Francis, London
- Morbidelli A., Levison H. F., Tsiganis K., Gomes R., 2005, *Nature*, 435, 462
- Murray C. D., Dermott S. F., 1999, *Solar System Dynamics*. Cambridge Univ. Press, Cambridge, p. 97
- Murray N., Holman M., 2001, *Nature*, 410, 773
- Murray N., Holman M., Potter M., 1998, *AJ*, 116, 2583
- Namouni F., Murray C. D., 2000, *Celest. Mech. Dyn. Astron.*, 76, 131
- Namouni F., Christou A. A., Murray C. D., 1999, *Phys. Rev. Lett.*, 83, 2506
- Nesvorný D., Dones L., 2002, *Icarus*, 160, 271
- Nesvorný D., Morbidelli A., 1998, *AJ*, 116, 3029
- Nesvorný D., Vokrouhlický D., 2009, *AJ*, 137, 5003
- Nesvorný D., Vokrouhlický D., Morbidelli A., 2013, *ApJ*, 768, 45
- Robutel P., Bodossian J., 2009, *MNRAS*, 399, 69
- Robutel P., Gabern F., 2006, *MNRAS*, 372, 1463
- Shankman C. J., 2012, M.Sc. thesis, The University of British Columbia
- Sheppard S. S., Trujillo C. A., 2006, *Science*, 313, 511
- Sheppard S. S., Trujillo C. A., 2010, *ApJ*, 723, L233
- Standish E. M., 1998, *JPL Planetary and Lunar Ephemerides*, DE405/LE405, Interoffice Memo. 312.F-98-048, Jet Propulsion Laboratory, Pasadena, California
- Stockwell J. N., 1873, *Smithsonian Contributions to Knowledge*, vol. XVIII, art. 3, p. xiv
- Verrier P. E., Evans N. W., 2008, *MNRAS*, 390, 1377
- Verrier P. E., Evans N. W., 2009, *MNRAS*, 394, 1721
- Wiegert P., Innanen K., Mikkola S., 2000, *AJ*, 119, 1978
- Winter O. C., Murray C. D., 1997, *A&A*, 328, 399
- Yoshida F., Nakamura T., 2005, *AJ*, 130, 2900
- Zhang S.-P., Innanen K. A., 1988a, *AJ*, 96, 1989
- Zhang S.-P., Innanen K. A., 1988b, *AJ*, 96, 1995